Cre/*lox*-mediated chromosomal integration of biosynthetic gene clusters for heterologous expression in *Aspergillus nidulans*

Indra Roux[1], Yit-Heng Chooi[1]

[1] School of Molecular Sciences, University of Western Australia, Perth, WA 6009, Australia.

Correspondence to: yitheng.chooi@uwa.edu.au

Abstract

Building strains for stable long-term heterologous expression of large biosynthetic pathways in filamentous fungi is limited by the low transformation efficiency or genetic stability of current methods. Here, we developed a system for targeted chromosomal integration of large biosynthetic gene clusters in *Aspergillus nidulans* based on site-specific recombinase mediated cassette exchange. We built *A. nidulans* strains harbouring a chromosomal landing pad for Cre/*lox*-mediated recombination and demonstrated efficient targeted integration of a 21.5 kb heterologous region in a single step. We further evaluated the integration at two loci by analysing the expression of a fluorescent reporter and the production of a heterologous polyketide. We compared chromosomal expression at those landing loci to episomal AMA1-based expression, which also shed light on uncharacterised aspects of episomal expression in filamentous fungi. This is the first demonstration of site-specific recombinase-mediated integration in filamentous fungi, setting the foundations for the further development of this tool.

Keywords: biosynthetic gene clusters, recombinase mediated cassette exchange (RMCE) , synthetic biology, Cre/*loxP* , heterologous expression , filamentous fungi, secondary metabolite, natural product

Abbreviations: BGCs, biosynthetic gene clusters ; HR, homologous recombination ; LE/RE, Left/Right recombination; LP, landing pad; PKS, polyketide synthase; RMCE, Recombinase Mediated Cassette Exchange; SM, secondary metabolite.

Introduction

Filamentous fungi are prolific producers of metabolites and enzymes with biotechnological applications in pharmaceutical, agricultural and food industries.[1,2] Importantly, fungal secondary metabolites (SMs) remain a promising source of novel drug leads.[3] The genes required to produce a SM are usually colocalised in the genome forming biosynthetic gene clusters (BGCs), which can be easily identified bioinformatically. However,

a large fraction of BGCs remain silent or lowly expressed under standard culture conditions, which limits their analysis.[3] As novel BGCs are often found in fungal species that are difficult to cultivate or engineer, heterologous expression in hosts with more genetic tools available is preferred.[4]

Filamentous fungi hosts present several advantages for the heterologous expression of BGCs from other filamentous fungi, such as increased compatibility of promoters and intron splicing, and their natural capability for producing SMs. In particular, *Aspergillus nidulans* has been widely used to produce SMs by chromosomal integration or episomal expression of heterologous BGCs.[4–6] Episomal systems based on the replicator AMA1 have facilitated initial testing of BGC products due their high transformation efficiency compared to integrative vectors.[7–9] However, the phenotypic stability of AMA1-vectors has been shown to be limiting, even under selective conditions.[10] Therefore, chromosomal expression is preferred for large-scale long-term stable bioproduction in industrial settings.[11] Additionally, strains with chromosomally encoded genes can be grown in low-cost complex substrates, such as spent grains, molasses or other agri-food residues [12], as they do not require maintaining selection pressures.

Currently, targeted chromosomal integration in *A. nidulans* is pursued through homologous recombination (HR) facilitated by strains deficient in the non-homologous end joining pathway (*nkuA*Δ).[13] However, HR efficiency drops when integrating large constructs.[11] As a result, HR-mediated integration of large BGCs relies on the laborious step wise integration of smaller BGC fragments.[14,15] To leverage the increasing amount of BGCs identified in novel fungi, new methods are needed for the fast creation of strains for heterologous BGC expression.[16]

Here, we develop a Cre/*lox* site-specific recombinase system for one-step chromosomal integration of BGCs in the heterologous host *A. nidulans*. Site specific recombinases are well suited for the integration of large DNA regions, as they mediate the strand exchange between the recombination sites in a size independent manner.[17] As Cre/*loxP* recombination is reversible, strategies for irreversible integration rely on mutated *lox* sites, either on its 8-bp asymmetric core or 13-bp palindromic arms. Heteromeric *lox* sites contain nucleotide variations in the left or right arms, respectively named LE and RE.[18] LE/RE integration relies on a single recombination event between a chromosomal *lox* site and the donor vector, but results in the integration of the complete donor vector (Figure 1). Another strategy for integration relies on two sequential recombination events between two pairs of heterospecific *lox* sites (harbouring mutations in the core) named Recombinase Mediated Cassette Exchange (RMCE). In RMCE the chromosomal landing pad is flanked by two *lox* sites that are incompatible between themselves but compatible with the sites flanking the genes of interest

located in the donor vector. In the presence of the Cre recombinase, the donor vector is integrated at the landing pad while in a second recombination event the donor vector backbone and the first landing pad cassette are excised, resulting on the irreversible integration of the genes of interest (Figure 1). RMCE has been used for the integration of large constructs in a wide range of cell factories and model organisms.[19–23] However, to this date there is no system for site-specific recombinases-mediated chromosomal integration in filamentous fungi.

Cre/*lox* recombination has been widely used in filamentous fungi for the excision of marker genes.[24–31] Here, we demonstrate Cre/*lox*-mediated integration is an efficient alternative for the integration of large heterologous constructs in *A. nidulans*, with potential to be expanded to other filamentous fungi.

Results

Design and construction of a recombinase-mediated integration system in *Aspergillus nidulans*

Cre/*lox*-mediated irreversible integration can be achieved by different strategies such as RMCE or LE/RE, making use of different engineered *lox* sites.[18] To simultaneously evaluate the feasibility of RMCE and LE/RE based chromosomal integration in *A. nidulans* we designed a combined strategy (Figure 1). We designed *lox* sites that contained both the heterospecific mutation of *lox2272* [32] and either of the heteromeric mutations of *lox71* and *lox66* [33], creating the sites *lox2272-71* and *lox2272-66* (Table S1). In principle, *lox2272-71* and *lox2272-66* recombination is irreversible as it results in the double LE/RE mutant site *lox2272-72* and *lox2272* (Table S1). Additionally, those sites are incompatible with *loxP* for recombination. By flanking the donor cassette and landing pad by *loxP* and either *lox2272-71 or lox2272-66,* the system can also be used for RMCE (Figure 1).

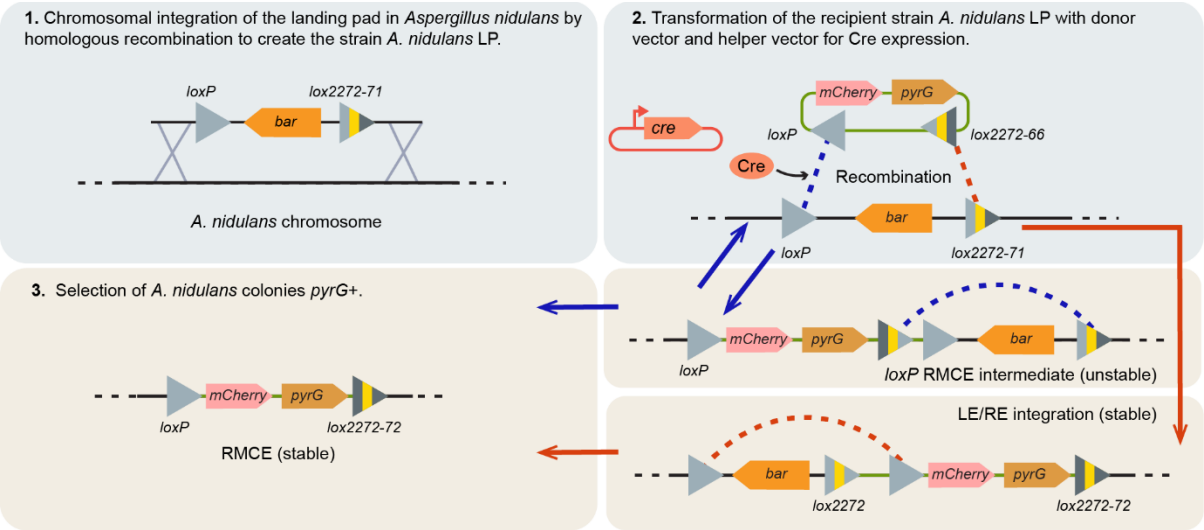

Figure 1 Overview of the strategy for Cre/*lox*-mediated chromosomal integration. **1)** The landing pad (LP) containing the *bar* marker gene flanked by *loxP* and *lox2272-71* is integrated in the destination locus of *Aspergillus nidulans* genome by homologous recombination. The resultant strain *A. nidulans* LP is used to prepare protoplasts that can be stored for subsequent transformations. **2)** *A. nidulans* LP protoplasts are transformed with the donor vector that contains *loxP* and *lox2272-66* flanking the marker gene *pyrG*, a fluorescent reporter and the genes of interest, along with a second vector for transient expression of *cre* recombinase. Stable integration can be achieved by LE/RE in 1-step recombination or in 2-steps by RMCE. **3)** Selection of the recombinant colonies in minimal media for *pyrG* complementation.

First, we validated the capability of Cre to recombine the sites *lox2272-66 and lox2272-71* by an assay *in vitro* (Figure S1). To create the recipient fungal strain, we chromosomally integrated the floxed (flanked by *lox* sites) landing pad (LP) by homologous recombination in the strain *A. nidulans* LO8030.[34] The landing pad consisted of the sites *loxP* and *lox2272-66* (Figure 1, Table S1) flanking the marker *bar* for glufosinate resistance. We selected as a first landing locus the sterigmatocystin (*stc*) biosynthetic gene cluster boundaries located in *A. nidulans* chromosome IV, as we previously used this locus for chromosomal expression of other genes.[35] After glufosinate selection of the transformant colonies and PCR verification, the strain *A. nidulans* landing pad 1 (LP1) was isolated for future tests.

For transient Cre recombinase expression, we created a helper vector unable to replicate in *A. nidulans.* The helper vector encodes a cassette for constitutive expression of Cre under the promoter *gpdA* (P_{gpdA}) and the terminator *trpC* (Figure 1). As the recipient strain *A. nidulans* LP1 carries *nkuA*Δ, which minimises random integration events, the helper vector presumably would be lost during fungal growth.[13]

To test the feasibility of RMCE/LE-RE integration at LP1, we built different donor vectors containing the fluorescent reporter *mCherry* and the *pyrG* marker flanked by *loxP* and *lox2272-71* (Figure 1, Figure S2A). Donor vector 1 is 6.6 kb long while donor vector 2 is a 12.2 kb shuttle vector that supports optional transformation-associated recombination cloning in *Saccharomyces cerevisiae*. Donor vector 2 also contains within the floxed region four cloning sites for the expression of biosynthetic genes under strong alcohol inducible promoters, derived from the vector pYFAC-CH2[8] (Figure S2A). As the four-promoter multiple cloning site is flanked by EcoRI sites, donor vector 2 can also be used for cloning genomic fragments containing a BGC. To demonstrate the utility of donor vector 2, we used it to clone an 18 kb region of *Aspergillus burnettii* by isothermal assembly, resulting in a 21.7 kb floxed donor region. This vector, named donor vector 2-bue contains six genes responsible for the biosynthesis of the polyketide compound **1**, a burnettiene precursor which will be described elsewhere (Figure S2A). As burnettienes are produced in *A. burnetti* (*bue* cluster is not silent), we hypothesised that if the *bue* genes were chromosomally integrated at a good expression

locus in *A. nidulans* we would observe the production of compound **1** as proof-of-concept (Figure S2B).[36]

Evaluation of recombination efficiency across different donor vectors

To evaluate the efficiency of the recombination system, we transformed protoplasts of *A. nidulans* LP1 by a small-scale PEG mediated transformation in 2 mL microtubes (approximately 5×10^6 protoplasts) (Figure 2A). We tested different amounts and ratios for each donor vector and the helper vector, and we also transformed the donor vector alone as control. We consistently obtained transformant colonies in the strains cotransformed with the helper vector for *cre* expression (3–13 colonies per transformation event) (Table 1). The variation in the number of transformant colonies was independent of the size of the transformant vector, which is expected for recombinase-mediated integration (Table 1). [21]

In the control strains without *cre* helper vector we mostly observed only small "abortive" colonies that did not support further growth. Abortive colonies arising from residual non-integrated vector encoding *pyrG* have been previously reported in *A. nidulans* Δ*nkuA.*[13] Interestingly, we observed a higher number of abortive colonies when transforming the smaller donor vector 1 compared to the larger donor vector 2 and donor vector 2-*bue*. Additionally, we did not observe viable colonies in the controls when transforming the larger donor 2 and donor 2-*bue* (Table 1).

To evaluate the mechanism of integration in the transformant *pyrG*+ colonies, we analysed the landing locus by PCR amplification of the recombination junction regions (Figure 2, Figure S3). The screening strategy consisted in four PCR tests per sample, designed so one primer would bind either neighbouring region at the 5′ or 3′ from the landing locus and the other primer would bind inside of the floxed region from either the original landing pad or recombination product (Figure 2B, Figure S3A). The expected amplicon size is ~1.5 kb in all PCRs and is indicative of recombination or presence of the original landing pad for each *lox* site (Figure 2C, Figures S3C–D). We verified representative PCR amplicons by Sanger sequencing, which confirmed *in vivo* that the recombination product between *lox2272-66* or *lox2272-71* is the double LE/RE mutant site *lox2272-72* (Figure 2D).

Analysing the total of transformant colonies per experiment, the frequency of successful recombinase-mediated integration ranged 29–100% across experiments (Table 1). We observed that lower recombination efficiency was found in transformations carried out with ≤0.9 pmol of helper vector. At higher amounts of helper vector transformed (≤1.5 pmol), Cre-mediated recombination efficiency for donor vector 1 ranged 60–83% (Table 1). Importantly, the recombination efficiency of the larger vectors donor 2, and donor 2-bue ranged a 90–100% at the highest helper vector concentrations (Table 1, Figures S3C–E). The lower frequency of

false positives seems to indicate that larger donor vectors are less prone to random integration.

Table 1 Overview of Cre/*lox*-mediated integration experiments in *Aspergillus nidulans*, with controls. Landing pad (LP) parent strain is indicated.

Donor vector	LP	Transformation event	Donor (pmol[a])	Helper (pmol[a])	Colonies with Cre-mediated integration from total[b]
Donor vector 1 (6.6 kb)	LP1	1	0.63	2.41	3/5 (60%)
		2	1.10	1.67	5/6 (83%)
		3	0.37	0.83	2/7 (29%)
		C1	1.10	-	0/1 (0%)
		C2	0.37	-	0/1 (0%)
Donor vector 2 (12.2 kb)		1	0.94	1.67	12/13 (92%)
	LP1	C1	0.94	-	No colonies[c]
Donor vector 2-*bue* (27.2 kb)	LP1	1	0.53	1.67	9/9 (100%)
		2	0.64	1.67	5/5 (100%)
		3	0.64	0.33	1/3 (33%)
		C1	0.53	-	No colonies[c]
		C2	0.64	-	No colonies[c]
		C3	0.64	-	No colonies[c]
	LP2	1	0.47	2.25	4/4 (100%)
		2	0.47	2.25	3/3 (100%)
		C1	0.47	-	No colonies[c]

[a] Estimated based on vector size and vector concentration obtained by Nanodrop after standard miniprep, which might overestimate DNA concentration.
[b] Per reaction 3–6×10^6 *A. nidulans* protoplasts were used.
[c] No viable colonies. Abortive colonies were inoculated in fresh media, but no growth was observed.

When analysing the recombination outputs (RMCE, LE/RE, *loxP* intermediate), we observed variable results across experiments and donor vectors (Figure 2E, Figure S3B). Overall, around half of the colonies that recombined at LP1 presented complete RMCE (N=17), while the rest were the intermediates LE/RE (N=6) and *loxP* (N=14) (Table 1). While *loxP* recombination is reversible, in the absence of Cre recombinase activity this intermediate should be stable. When analysing all experiments by PCR for presence of the *cre* gene we obtained PCR positive results in several colonies across experiments (Figure S4). These results could imply that random integration of the *cre* helper vector occurs in *A. nidulans* or that traces of the residual vector might be present at later growth stages.

Our screening strategy consisted in testing for the presence of recombination product along with presence or absence of the original landing pad (Figure 2A, Figure S3A). Our results seem to be indicative of genetic heterogeneity in the primary colonies, as a big proportion of transformant strains gave positive PCR result for the recombination product as

well as the original landing pad (Figures S3C–E). If the first recombination event happened at a later polynuclear developmental stage the primary colonies could be heterokaryon, requiring subsequent isolation by restreaking on selective conditions. At this stage, we decided to proceed by investigating the phenotypic stability of the transformant colonies by analysing the reporter genes.

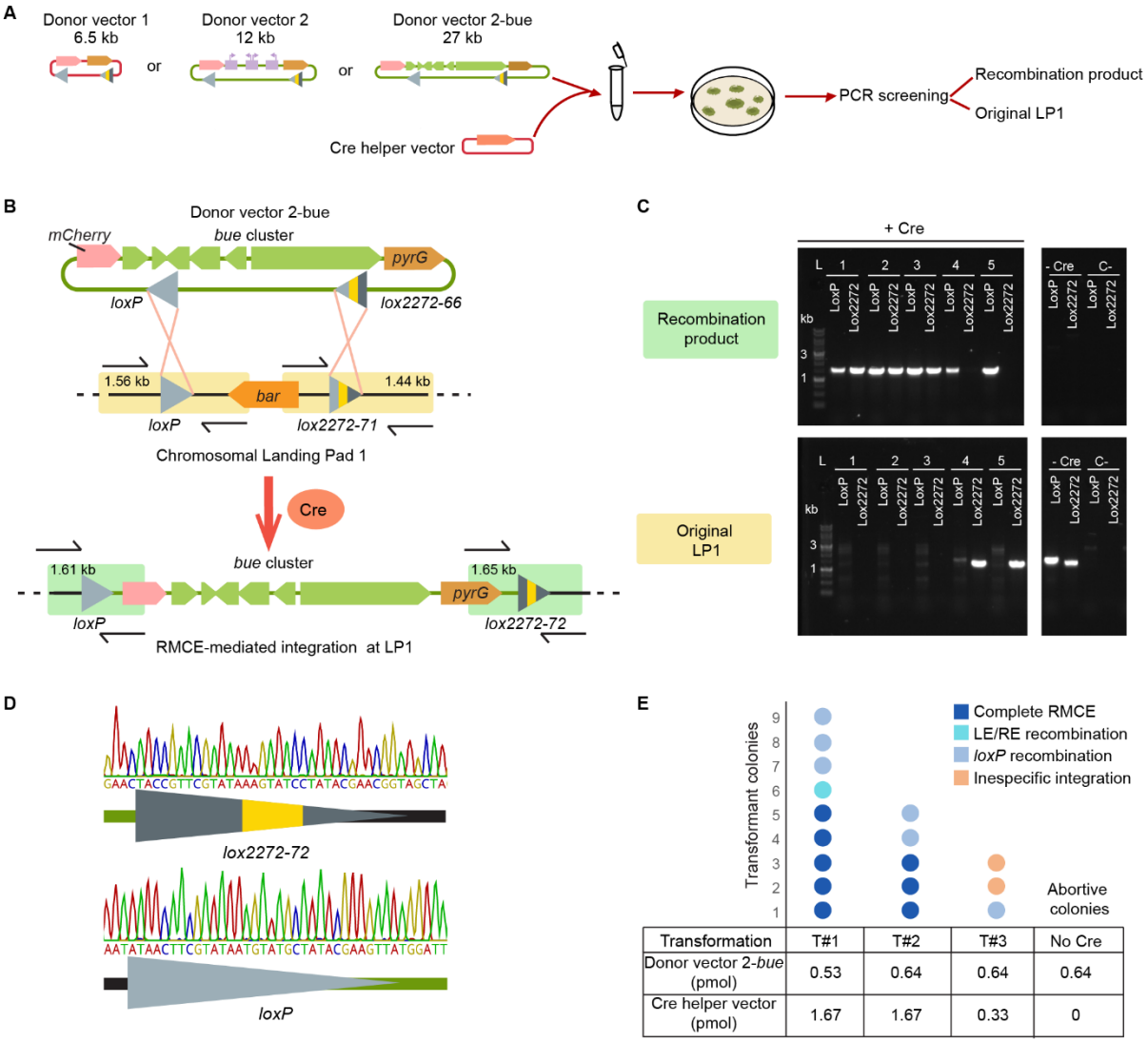

Transformation	T#1	T#2	T#3	No Cre
Donor vector 2-*bue* (pmol)	0.53	0.64	0.64	0.64
Cre helper vector (pmol)	1.67	1.67	0.33	0

Figure 2. Efficient targeted chromosomal integration of a large heterologous biosynthetic gene cluster in *Aspergillus nidulans* **A.** Experimental setup schematic for the evaluation of donor vectors (6.5–27 kb donor vectors with 3–21 kb inserts). **B.** Schematic of *bue* cluster genes integration strategy at landing pad 1 (LP1). Primer binding sites and PCR regions used for screening are indicated in the scheme with the amplicon sizes indicated. Schematic not at scale. **C.** Representative gel of the PCR results of a transformation event with donor vector 2-*bue*, different transformant colonies are indicated as numbers. Complete gel is found in Figure S3. **D.** Confirmation of the expected recombination event by Sanger sequencing of representative screening PCRs. **E.** Amount of transformant colonies obtained in different transformation experiments with donor 2-bue, with the integration mechanism indicated as a colour code, as analysed by PCR. Recombination is obtained across a different amount and proportion of donor vector and Cre helper vector.

Evaluating expression at landing pad 1 with a fluorescent reporter and metabolite production

To evaluate the strains with recombinase-mediated integration at LP1, we first analysed the expression of the fluorescent reporter mCherry encoded in the donor cassette. To benchmark chromosomal expression at LP1, we compared this expression system to strains expressing mCherry from episomal AMA1-pyrG vectors. We consistently observed fluorescence in mycelia of colonies with mCherry integrated at LP1 compared to the negative control (Figure 3A, Figure S5). However, fluorescence in strains with mCherry integrated at LP1 was low compared to the AMA1-encoded counterpart under selective conditions. We also observed that when hyphae from strains harbouring AMA1-pyrG encoded P_{gpdA}-*mCherry* were grown in non-selective conditions, some hyphae retained higher fluorescence than their LP1-integrated counterpart (Figure 3A, Figure S5).

Inspired by comparative studies of chromosomal and episomal expression in yeast by Jensen *et al.* [37], we analysed the spores of recombinant colonies by flow cytometry to test phenotypic stability. We observed a unimodal distribution of fluorescence in the strains with *mCherry* integrated at LP1, distinguishable from the negative control (Figure S6A). The strains with AMA1-based episomal expression of *mCherry* presented a much wider multimodal distribution (Figure S6A), which is expected due to the phenotypic instability of AMA1-encoded genes on spores even under selective conditions.[10] While these results indicated that chromosomal expression at LP1 results in a more homogeneous cell population, expression at LP1 is at least one order of magnitude below the signal from the best performer spores of AMA1-episomal expression. Overall, our analysis of the fluorescent reporter at LP1 by flow cytometry and microscopy supported phenotypic stability, which is expected of chromosomally integrated gene.

To assess compound production at LP1, we cultivated different transformant strains of Cre/*lox*-mediated integration of donor vector 2-*bue* (N=9) (Figure S7). However, we did not observe detectable compound production when the genes were integrated at LP1, while we consistently observed production of compound **1** in the strains with episomal expression (N=8) (Figure S7).

Overall, when evaluating fluorescent reporter mCherry and compound **1**, expression at LP1 was lower than its episomal counterpart. Furthermore, the lack of compound production at LP1 makes it not an ideal locus for BGC expression for natural product discovery. To make our recombinase-mediated integration system more useful, we decided to evaluate integration at a landing locus previously validated for production of heterologous compounds.

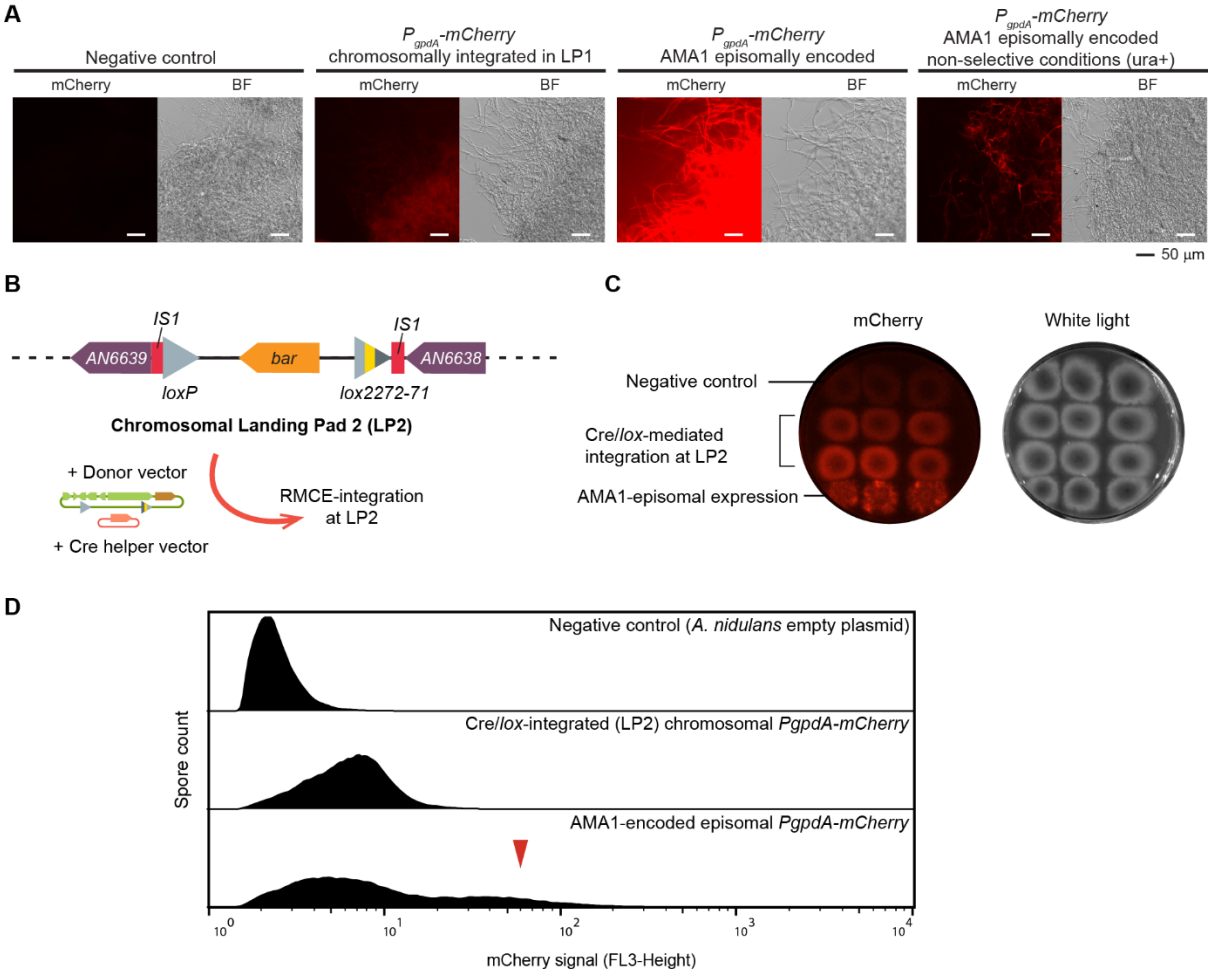

Figure 3. Chromosomal expression of mCherry after recombination compared to AMA1-based episomal expression. **A.** Analysis of fluorescence in mycelia after overnight culture in liquid media. Strains with *mCherry* chromosomally integrated at LP1 show lower fluorescence than the AMA1-based episomal counterpart under selective conditions. Selection pressure is needed to support high AMA1-based episomal expression. Samples with similar mycelial growth were observed under mCherry filter and brightfield (BF) by fluorescence microscopy. Scale bar 50 µm. Biological replicates are found in Figure S5. **B.** Overview of the strategy to evaluate the site landing pad 2 at *Aspergillus nidulans* IS1 locus. **C.** Analysis of colony growth by fluorescence photography shows a patchy pattern in the fluorescence of colonies with AMA1-based expression under selective conditions, compared to more homogeneous fluorescence in strains with chromosomal expression at LP2. Extended information at Figure S9. **D**. Analysis of spores by flow cytometry shows more compact and homogeneous fluorescence in samples with chromosomal integration of *mCherry* at LP2 compared to AMA1-based episomal expression. A proportion of the spores expressing mCherry episomally from AMA1 vectors can reach fluorescence levels one order of magnitude higher than spores with chromosomal expression at LP2 (see red arrow). Biological replicates, event counts and gating strategy can be found in Figure S6.

Construction and evaluation of landing pad 2

The site *IS1* located in *A. nidulans* chromosome I has been used as target for integration of heterologous biosynthetic genes by homologous recombination, for example the geodin BGC.[14] We proceeded to integrate our floxed landing pad at *IS1* by HR, creating the strain *A.*

nidulans LP2 (Figure 3B, Figure S7A). Next, we evaluated recombinase-mediated integration at LP2 of Donor vector 2-*bue* (Figure S7). In both transformations tested we obtained 100% efficiency of recombinase-mediated integration, with complete or intermediate RMCE, as evaluated by diagnostic PCR (Table 1, Figure S7B–C).

At this stage we also evaluated the use of a replicative AMA1-based vector containing the floxed *pyrG* cassette as donor vector 3 (Figure S8). However, we did not obtain evidence of recombination with this prototype, which highlights the relevance of selecting for the recombination event and not just DNA uptake (Figure S8).

To evaluate expression at LP2, we first assessed expression of the fluorescent reporter mCherry. Inspired by Vanegas *et al*, where an mCherry reporter integrated at *IS1* was assessed with fluorescent photography we first evaluated the transformant colonies by a similar method.[38] In our assay, we replicated transformant colonies in solid media under selective and non-selective conditions and benchmarked it against AMA1-based expression (Figure 3C, Figure S9). We observed that the strains with chromosomal integration of mCherry at LP2 showed uniform fluorescence in selective and non-selective conditions, distinguishable from the negative control. Interestingly, the strains with AMA1-encoded mCherry presented a patched expression pattern on the conidia on the colony surface with some regions displaying high fluorescence under both selective and non-selective conditions (Figure S9A). To further investigate the pattern of AMA1-based mCherry expression, we performed a spore dilution and plated under selective and non-selective conditions (Figure S9B). We observed that in non-selective supplemented media we obtained a mixture of colonies with no noticeable fluorescence along with colonies with observable patchy fluorescence. Interestingly, the colonies with fluorescence in non-selective media were comparable to the colonies under selective conditions.

To further analyse the profile of mCherry expression at LP2, we analysed spores from different transformant colonies by flow cytometry. We observed a similar pattern than the strains with mCherry integrated at LP1 (Figure 3D, Figure S6). These results indicate that P_{gpdA}-*mCherry* integrated at either LP2 or LP1, failed to achieve the fluorescence levels comparable to the best performer spores in the multicopy AMA1-encoded P_{gpdA}-*mCherry.* We also observed lower fluorescence in mycelia from strains with chromosomal expression at LP2 compared to AMA1-based episomal counterpart (Figure S5).

Next, we evaluated the production of compound **1** in the *A. nidulans* strains with *bue* genes integrated at LP2. After cultivation, like the strains with *bue* genes integrated at LP1, we did not observe production of compound **1** in the recombinant strains (N=5) when analysing media extracts (Figure S10A). For troubleshooting, we verified that the end of culture fungal

pellets expressed mCherry (Figure S10A). As a next troubleshooting step, we investigated two transformant strains with *bue* genes integrated at LP2 and one at LP1 by whole genome sequencing (Figure S11). We confirmed the expected recombination with no mutations that could explain the lack of compound production. Thus, the lack of compound production could be due to the *bue* genes being silent when integrated chromosomally.

Activation of chromosomally integrated *bue* genes by transcription factor overexpression

As the strains with chromosomal integration of *bue* genes at LP1 or LP2 did not produce compound **1**, we hypothesised that overexpression of the *bue* cluster specific transcription factor (TF) *bueR* could activate the cluster in chromosomal context.

For each landing locus, we selected a representative transformant strain with the *bue* genes integrated by RMCE and prepared protoplasts (Figure 4B,C). After transformation with the vector *pYFAC-*P_{gpdA}*-bueR-bueG (Ref),* we observed that the strains overexpressing the TF BueR presented production of compound **1**, while the control strains with an empty vector did not present compound production (Figure 4). This result validates that the strains had integrated a functional and complete copy of the *bueA/B/C/D/E/R*. When comparing the strains with *bue* genes integrated at LP1 and LP2, we observed similar production levels between them (Figure 4C).

One of the benefits of chromosomal expression is that cultures can be grown under non-selective conditions without compromising productivity. For simplicity, in previous small scale culturing experiments we cultivated the strains on liquid minimal media with no uracil and uridine, the selective condition of the *pyrG* marker. To evaluate expression under non-selective conditions, we cultivated replicates from the strains containing the *bue* genes at LP2 and TF overexpression in media supplemented with uracil and uridine. It should be noted that the AMA1-based vector for TF expression is under the selection of pyridoxal auxotrophy with the *pyroA* marker and the medium used lack pyridoxine. As expected, the uracil and uridine selection pressure was not needed for compound production (Figure 4B). Interestingly, we observed 3-fold higher production in the strains grown in non-selective conditions (Figure 4C). Positional effects arising for insufficient expression of the *pyrG* marker integrated in some loci have been observed in *A. nidulans* before, however changes in compound production in uracil/uridine supplemented media could be due other effects.[39,40]

To sum up, overexpression of the cluster specific TF allowed to activate the expression of *bue* genes at two different chromosomal contexts. These results demonstrate that recombinase-mediated integration is a feasible strategy to build strains for heterologous

compound production, but that alternative strategies might be needed for BGC activation it the cluster remains silent. Overall, chromosomal expression permitted cultivating in non-selective media without compromising yields.

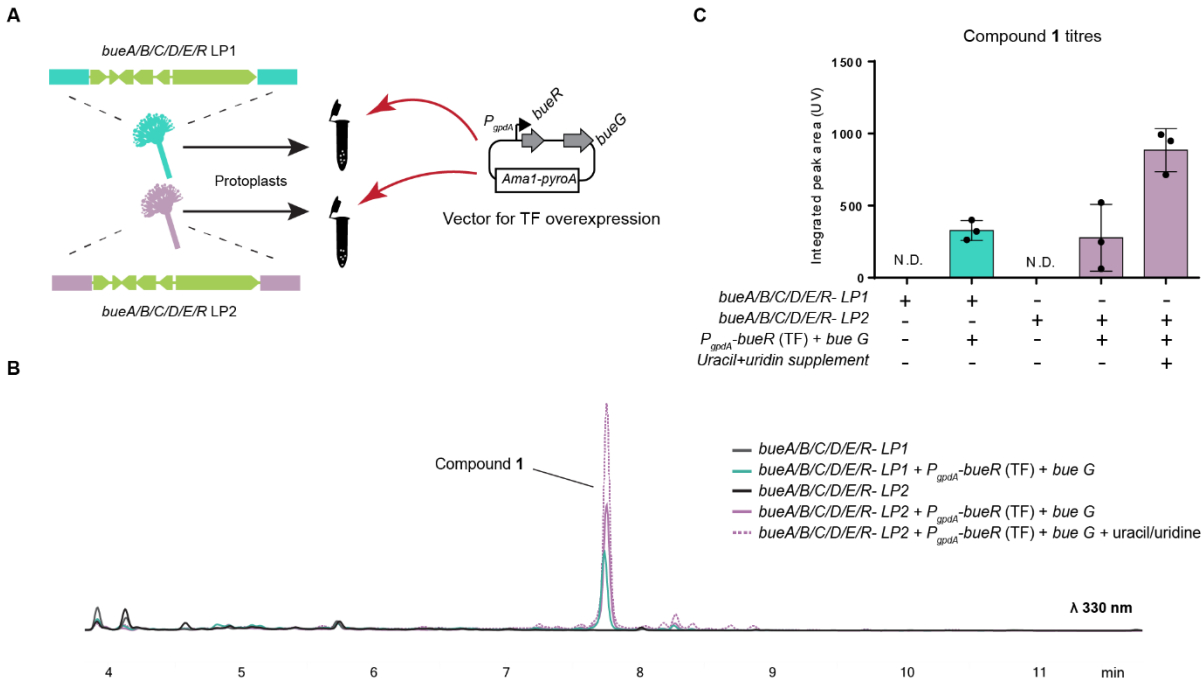

Figure 4. Activation of chromosomally integrated *bue* cluster genes by transcription factor overexpression. **A.** Experimental approach. Protoplast were prepared from strains with RMCE integrated *bue* genes at LP1 or LP2, and further transformed with a vector containing the construct P_{gpdA}-*bueR* for transcription factor (TF) overexpression and *bueG* encoding a transporter. **B.** Chromatogram traces at 330 nm show activation of compound **1**production on strains with transcription factor overexpression. **C.** Quantification of compound **1** production show comparable compound levels in the strains with the genes integrated at LP1 or LP2 with TF overexpression on minimal media. Strains grown on media supplemented with uracil and uridine (non-selective condition) presented higher titres than the same strain grown on minimal media (selective condition). Calculated integrated peak area values are the mean of three biological replicates; specific values are indicated as black dots, and error bars represent SD. Two-sided Welch's T-test P-value≥0.024 .

Discussion

In this work we designed, built, and tested a system for Cre/*lox*-mediated chromosomal integration of long DNA fragments for the heterologous expression of BGCs in *A. nidulans*. Site-specific recombinase mediated integration represents a relevant expansion to the synthetic biology toolbox for filamentous fungi, where recombinases had only been used for gene deletion or inversion.[31] The vector set developed in this work has the potential to be easily adapted for integration at different chromosomal landing loci or related fungal chassis.[41]

We demonstrated targeted one-step integration of long DNA regions of up to 27 kb by LE/RE and 21 kb by RMCE in *A. nidulans*. We obtained high transformation efficiency (up to 100%) using a small-scale transformation protocol with optimised amounts of helper vector.

We additionally observed that the false positive rate and the presence of abortive colonies diminished when transforming large donor vectors (≥12 kb), making this system particularly advantageous for integration in the size range where HR efficiency drops. We also demonstrated that the resulting strains with chromosomally encoded genes presented a more uniform fluorescence phenotype in spores and mycelia compared to AMA1-encoded genes, evidencing genetic and phenotypic stability.

The developed Cre/*lox*-mediated integration system presents an advantageous alternative to HR for the single-step integration of large constructs. However, it also faces the same constraints as HR for heterologous expression featuring a single gene copy in a chromosomal context. When integrating the heterologous genes *bueA/B/C/D/E/F/R* under their native promoter at LP1 or LP2 initially we did not observe compound production, unlike the episomal counterpart. Nevertheless, when overexpressing the cluster specific TF *bueR* we restored compound production from biosynthetic genes at LP1 and LP2. Strategies for BGC activation, such as TF overexpression, promoter replacement or CRISPRa could be used to activate chromosomally integrated genes that remain silent.[35] Alternatively, integration in a better locus for expression could also result in improved performance.

By benchmarking chromosomal expression to AMA1-*pyrG* based expression, this work also represents an unprecedented characterisation of many other aspects of AMA1-*pyrG* episomal expression in *A. nidulans*. We analysed episomal expression in fungal growth in both solid media and submerged liquid culture, which have different morphological and developmental characteristics. While *A. nidulans* grown in solid media completes the developmental stages that lead to sporulation, fungal growth in liquid submerged culture gets arrested in an undifferentiated hyphal state with almost no conidia production.[42,43] In the literature, AMA1 expression is usually characterised by observing the phenotype of spores grown on solid selective media.[4,10] Our original analysis of AMA1-pyrG phenotypic stability by flow cytometry adds a quantitative estimation of the phenotypic heterogeneity of AMA1-based expression in spores from in *A. nidulans* grown under selective conditions in solid media. This is particularly relevant considering the impact of spore expression in fungal development.[44] Even though our results indicate that the phenotypic stability of AMA1-encoded genes in spores is limited, we observed that during mycelial growth in liquid culture there is a more prevalent phenotype for strong expression, as evidenced by fluorescence and compound production.

Lastly, the Cre/*lox*-mediated integration platform in *A. nidulans* can be expanded in future works. Cre-mediated integration could be particularly relevant for building strains for heterologous expression of large genomic regions containing BGCs cloned by genome capture.[9] The current system could also be upgraded for simultaneous integration in different

loci by using multiple landing pads with different heterospecific recombination sites. Different strategies could also be evaluated to optimise the delivery of Cre recombinase, such a self-excising Cre expression cassettes.[22] The use of a split *pyrG* marker between recombination sites could be evaluated to minimise the background by random integration and abortive colonies, or to further evaluate AMA1-based donor vectors.[45]

To sum up, Cre/lox-mediated integration of BGCs has the potential to speed up the process of constructing strains to produce heterologous metabolites in *A. nidulans.* The capability to uptake and maintain complex exogenous DNA is a key requirement for a good chassis organism for bioproduction [46]. Thus, this system can be used to upgrade other filamentous fungi chassis.

Methods

Vector Construction

All the oligonucleotides used for vector construction are listed in Appendix 1 Table 7.6 with their destination vector indicated. The landing pad vector pGemLP1-loxP-bar-Lox2272-71 was built by a sequential cloning process: pBARGPE1 [47], obtained from the Fungal Genetics Stock Centre, was digested with PmlI and AatII and the site *lox2272-71* was created by ligation to the annealed oligonucleotides AattI-Lox2272-71Rv and AattI-Lox2272-71Fw. A fragment containing the marker *bar* flanked by *lox2272-71* and a *loxP* from pBARGPE1 was PCR amplified and cloned by isothermal assembly with NEBuilder HiFi DNA Assembly Master Mix (New England Biolabs, MA, USA) into NotI digested pGemT (Promega) incorporating at the 5′ and 3′ 1 kb homology arms for LP1 amplified from *A. nidulans* gDNA, creating the vector pGem-LP1. To build pGemLP2-loxP-bar-Lox2272-71, the floxed *bar* cassette was amplified from pGemLP1-loxP-bar-Lox2272-71, and two fragments containing the homology arms for LP2 were amplified from *A. nidulans* gDNA and cloned with NEBuilder HiFi DNA Assembly Master Mix into NotI digested pGemT.

Cre was amplified from pBF3038 [48] and cloned into pBARGPE1-LIC [49]. The P_{gpdA}-*Cre*-T_{trpC} cassette was then further amplified and cloned into pGemT creating pGem-PgpdA-Cre-TtrpC. The donor vector was initially built using a NotI and MscI digested pKW20088 [50], amplifying a ~200 bp fragment containing *loxP* from pXP322 [48] and creating the *lox2272-66* with a gBlock, resulting in the intermediate vector pKW20088-loxP-pyrG-lox2272-66. On parallel, the coding sequence of *mCherry* was amplified from pMP7601 [51] and cloned into pBARGPE1 under P_{gpdA}. pKW20088-loxP-mCherry-pyrG-lox2272-66 (donor vector 3) was created after PacI digestion of pKW20088-loxP-pyrG-lox2272-66 and isothermal assembly of a PCR amplicon containing P_{gpdA}-*mCherry*-T_{trpC}. pGem-loxp-lox71-2272 was created amplifying the floxed *pyrG* cassette from pKW20088-loxP-pyrG-lox2272-66 with primers that

added NotI sites in the ends of the amplicon and cloning by NotI digestion and ligation to NotI digested pGemT (Promega). pGem-loxp-mcherry-lox71-2272 (donor vector 1) was created with PacI digestion of pGem-loxp-lox71-2272 and amplification of P_{gpdA}-*mCherry*. pRecomb-loxp-mcherry-4Gcloningsite-lox71-2272-66 (donor vector 2) was created *de novo* by isothermal assembly of PCR parts containing the floxed cassette of pKW20088-loxP-pyrG-lox2272-66, the 4G cloning cassette from pYFAC-CH2 [8] and sequences from pKW20088 to include the sequences for plasmid maintenance and selection in *E. coli* and *S. cerevisiae*.

pRecomb-loxp-mcherry-BueABCDER-lox71-2272-66 (donor2-bue) was created digestion Donor2 with NotI and isothermal assembly of four PCR fragments containing the partial *bue* cluster, amplified from *A. burnetti* MST-FP2249 gDNA.

Aspergillus nidulans strains construction and transformation

A. nidulans parental strains with LP1 or LP2 were created by polyethylene glycol (PEG)-calcium-based transformation [52] with NotI linearized vectors pGemLP1-loxP-bar-Lox2272-71 or pGemLP2-loxP-bar-Lox2272-71 containing 1 kb homology regions at 5′ and 3′ of the floxed bar to facilitate homologous recombination in *A. nidulans* LO8030. Colonies were selected for resistance to glufosinate extracted from Basta (Bayer, Vic., Australia) [53] an the event was confirmed by diagnostic PCR.

Protoplasts of *A. nidulans* LO8030 LP1 or LP2 were prepared from germlings [52], mixed with a quarter volume PEG 60% to a final concentration of 10^8 protoplasts per mL and frozen at -80 °C for later use. AMA1-vectors were transformed into *A. nidulans* protoplasts modifying Lim *et al.* (2012) to minimize the required transformation volume. In a 2 mL microcentrifuge tube, 60 µL of thawed protoplast solution was incubated with 40 µL of STC buffer (1.2 M sorbitol, 10 mM $CaCl_2$, 10 mM Tris–HCl, pH 7.5) and the vector amounts indicated in Table 5.2 and across figures on the main text. After 20 min of incubation on ice, 400 µL of the calcium PEG 60% mix was added and mixed gently by inversion, followed by a 20 min incubation at room temperature. After adding 1 mL of STC buffer the mix was spread on SMM supplemented with pyridoxine and riboflavin but deficient in uracil for auxotrophic selection (u-p+r+), divided in two plates that were then incubated for three days at 37 °C to generate transformant colonies.

For the activation of the chromosomally integrated *bue* genes by TF overexpression, protoplasts were prepared from the strains *A. nidulans LO8030-LP1-bueA/B/C/D/E/R* and *A. nidulans LO8030-LP2-bueA/B/C/D/E/R.* Protoplasts were transformed with the vector pYFAC-bueG-PgpdA-bueR and selected on SMM u-r+p-.

Relevant strains were analysed by whole genome sequencing with the DNBSEQ-2000 PE150 platform at BGI Tech Solutions co. (BGI, Hong Kong), resulting in ~2 Gb of raw genome

data (150 bp, paired-end). The reads were mapped to chromosome sequences containing the expected recombination product using Geneious 11.03.

Diagnostic PCRs

For a more sensitive genotyping of the strains after recombination, gDNA of the transformant strains were extracted before PCR screening. Spores picked from individual colonies were grown overnight in liquid GMM U- at 37 °C for mycelial mass, that was grinded on liquid nitrogen and extracted by a clean-up with chloroform:isoamyl alcohol 24:1 followed by isopropanol precipitation. The PCR amplification was conducted by 3 min at 94 °C initial denaturing followed by 27 cycles of 30 s at 94 °C, 30 s at 56.5 °C, 60 s at 72 °C, in a thermocycler with Taq polymerase, using ~30 ng *A. nidulans* gDNA in a 10 µl reaction volume. The PCR products were run in a 0.8% agarose gel with 2 µl of the AccuRuler 1 kb DNA RTU Ladder (Maestrogen). All agarose gel images were acquired with a Vilber E-Box VX-2 gel imager.

Representative PCRs of recombination products were amplified with Pfu polymerase for Sanger sequencing and mapped to the expected recombination product with Geneious 11.03 to confirm the expected recombinant products.

In vitro validation of *lox* sites

The substrate DNA fragments were PCR amplified with primers LoxP-pyrG-F and GBlock-R from template vector pKW20088-loxP-pyrG-lox2272-66 and with primers LIC-H1-F and PbarUpstream-R-Seq from pGemLP1-loxP-bar-Lox2272-71. The *in vitro* recombination was performed following the protocol of Cre (NEB, M0298M), incubating at 1.30 h at 37 °C and heat inactivated. As control the PCR fragments were subject to the same treatment but without recombinase. The reaction products were run in a 0.8% agarose gel with 2ul of the AccuRuler 1 kb DNA RTU Ladder (Maestrogen) and the image was taken with a blue LED transilluminator and a phone camera.

Fluorescence microscopy

Spores from three or more individual colonies were picked and grown in small petri dishes containing liquid GMM u-p+r+, supplemented with pyridoxine and riboflavin to obtain mycelia. Samples were incubated at 37° C and grown overnight and submerged in mycelial wash ($MgSO_4$ 0.6M) before mounting the slides. Fluorescence images were captured at 20x on the epifluorescence inverted microscope Eclipse Ti2 (Nikon), using numerical aperture (NA) 0.75 and Plan Apo λ 20x objective lens (Nikon) and a Camera DS-Qi2 (Nikon) controlled by NIS Elements Advanced Research (Nikon). Fluorescent microscopy was carried out under a mCherry filter set (562/40 nm excitation, 593 nm dichroic beamsplitter, and 641/75 nm

emission), using a 400 ms exposure and 1.8x analog gain unless specified otherwise. Images were recorded using NIS-Elements Advanced Research software package (Nikon).

Flow cytometry

Spores were collected with a sterile loop from colonies grown for 3 days in solid GMM u-p+r+ and suspended in water. The spore suspension was carefully filtered through a syringe containing sterile cotton to remove residual mycelia and diluted to a concentration of ~1.10^6 spores/mL. Data acquisition was performed immediately after spore suspension using a FACSCalibur (BD Biosciences) flow cytometer operated with filtered water as shear fluid. mCherry signal was observed with a 488 nm excitation laser and the filter FL3 (≥670 nm) and 35,000 events were detected per measurement or 4 minutes of run were collected for the water control (no spore sample was run more than 4 minutes).

The data was processed using FlowJo V10 software (TreeStar). The output was gated according to FCS size to limit to the size range of spores, an example of the gating strategy is indicated on the Figure S6. Curves are presented as staggered histograms. Mean and SD was determined with the FlowJo software.

Fluorescent photography

Closed plates were analysed in ChemiDoc MP Imaging System (Bio-Rad). MCherry images were obtained using the excitation source Green epi illumination and the emission filter 605/50 nm with exposure time of 0.01 seconds. Bright field was captured with white illumination and a standard emission filter in automatic exposure. Images were recorded with ImageLab software (Bio-Rad).

Culture conditions and metabolic profile analysis by LC-DAD-MS

For each transformant strain, spores from individual colonies were picked for culture analysis and re-streaked individually in a solidified GMM -u-p+r+ plate to be cultivated for three days at 37 °C. Spores were harvested from plates in 1 mL of 0.1% Tween 80 (Sigma, MO, USA) and approximately 10^8 spores were inoculated into 250-mL flasks containing 50 mL liquid GMM u-p+r+ medium. Additionally, ampicillin was added to 50 µg mL^{-1}. Cultures were incubated for 4 days with shaking set to 200 rpm and 26 °C. At the end of the culture, 20 mL of media was collected in 50-mL falcon tubes by filtration with Miracloth (Milipore, MA, USA). The metabolites were extracted from the liquid culture with 20 mL of an organic solvent mixture containing ethyl acetate, methanol, and acetic acid (89.5:10:0.5 ratio). The crude extracts were dried down in vacuo and re-dissolved in 0.3 mL of methanol for LC-DAD-MS analysis.

The analyses of the metabolite profiles were performed on an Agilent 1260 liquid chromatography (LC) system coupled to a diode array detector (DAD) and an Agilent 6130 Quadrupole mass spectrometer (MS) with an electrospray ionization (ESI) source. In all cases

3 µL of the methanol dissolved crude extract was injected. Chromatographic separation was performed at 40 °C using a Kinetex C18 column (2.6 µm, 2.1 mm i.d. 3 100 mm; Phenomenex). Chromatographic separation was achieved with a linear gradient of 5–95% acetonitrile-water (containing 0.1% v/v formic acid) in 10 minutes followed by 95% acetonitrile for 3 minutes, with a flow rate of 0.70 mL min-1. The MS data were collected in the *m/z* range 100–1000 in negative ion mode and UV observed at DAD λ=330 nm.Peak areas were determined by peak integration of DAD λ=330 nm chromatogram using Masshunter Workstation Qualitative Analysis (Agilent).

Statistical analysis

Statistical analysis was performed with GraphPad Prism 8.3.0 by a Two-sided Welch's T-test using biological triplicates.

Acknowledgments

Y.H.C. and this project is supported by an ARC Future Fellowship (FT160100233). I.R. was recipient of an UWA PhD Scholarship. This research was funded, in part, by the Cooperative Research 418 Centres Projects scheme (CRCPFIVE000119). *Aspergillus burnettii* MST-FP2249 is a gift from Microbial Screening Technologies (MST) and *A. nidulans* LO8030 is a gift from Berl Oakley. We thank Hamideh Rezaee for her help building donor vector 2, and Julia Grassl (UWA) for helping us to set up the flow cytometer. We also thank members of Lister Lab (UWA), specifically Jahnvi Pflüger, for whole plasmid sequencing.

Author contribution

I.R and Y.H.C conceived the project and wrote the manuscript. I.R. designed and performed the experiments and the data analysis.

References

(1) Wakai, S.; Arazoe, T.; Ogino, C.; Kondo, A. Future Insights in Fungal Metabolic Engineering. *Bioresour. Technol.* **2017**, *245*, 1314–1326. https://doi.org/10.1016/j.biortech.2017.04.095.

(2) Meyer, V.; Basenko, E. Y.; Benz, J. P.; Braus, G. H.; Caddick, M. X.; Csukai, M.; de Vries, R. P.; Endy, D.; Frisvad, J. C.; Gunde-Cimerman, N.; Haarmann, T.; Hadar, Y.; Hansen, K.; Johnson, R. I.; Keller, N. P.; Kraševec, N.; Mortensen, U. H.; Perez, R.; Ram, A. F. J.; Record, E.; Ross, P.; Shapaval, V.; Steiniger, C.; van den Brink, H.; van Munster, J.; Yarden, O.; Wösten, H. A. B. Growing a Circular Economy with

Fungal Biotechnology: A White Paper. *Fungal Biol. Biotechnol.* **2020**, *7*, 5. https://doi.org/10.1186/s40694-020-00095-z.

(3) Keller, N. P. Fungal Secondary Metabolism: Regulation, Function and Drug Discovery. *Nat. Rev. Microbiol.* **2019**, *17*s, 167–180. https://doi.org/10.1038/s41579-018-0121-1.

(4) Anyaogu, D. C.; Mortensen, U. H. Heterologous Production of Fungal Secondary Metabolites in Aspergilli. *Front. Microbiol.* **2015**, *6*, 7. https://doi.org/10.3389/fmicb.2015.00077.

(5) He, Y.; Wang, B.; Chen, W.; Cox, R. J.; He, J.; Chen, F. Recent Advances in Reconstructing Microbial Secondary Metabolites Biosynthesis in *Aspergillus* Spp. *Biotechnol. Adv.* **2018**, *36* , 739–783. https://doi.org/10.1016/j.biotechadv.2018.02.001.

(6) Caesar, L. K.; Kelleher, N. L.; Keller, N. P. In the Fungus Where It Happens: History and Future Propelling *Aspergillus Nidulans* as the Archetype of Natural Products Research. *Fungal Genet. Biol.* **2020**, *144*, 103477. https://doi.org/10.1016/j.fgb.2020.103477.

(7) Liu, L.; Tang, M.-C.; Tang, Y. Fungal Highly Reducing Polyketide Synthases Biosynthesize Salicylaldehydes That Are Precursors to Epoxycyclohexenol Natural Products. *J. Am. Chem. Soc.* **2019**, *141*, 19538–19541. https://doi.org/10.1021/jacs.9b09669.

(8) Hu, J.; Sarrami, F.; Li, H.; Zhang, G.; Stubbs, K. A.; Lacey, E.; Stewart, S. G.; Karton, A.; Piggott, A. M. M.; Chooi, Y.-H. H. Heterologous Biosynthesis of Elsinochrome A Sheds Light on the Formation of the Photosensitive Perylenequinone System. *Chem. Sci.* **2019**, *10*, 1457–1465. https://doi.org/10.1039/c8sc02870b.

(9) Clevenger, K. D.; Bok, J. W.; Ye, R.; Miley, G. P.; Verdan, M. H.; Velk, T.; Chen, C.; Yang, K. H.; Robey, M. T.; Gao, P.; Lamprecht, M.; Thomas, P. M.; Islam, M. N.; Palmer, J. M.; Wu, C. C.; Keller, N. P.; Kelleher, N. L. A Scalable Platform to Identify Fungal Secondary Metabolites and Their Gene Clusters. *Nat. Chem. Biol.* **2017**, *13*, 895–901. https://doi.org/10.1038/nchembio.2408.

(10) Aleksenko, A.; Clutterbuck, A. J. Autonomous Plasmid Replication in *Aspergillus Nidulans* : AMA1 and MATE Elements. *Fungal Genet. Biol.* **1997**, *21*, 373–387. https://doi.org/10.1006/fgbi.1997.0980.

(11) Li, L.; Liu, X.; Wei, K.; Lu, Y.; Jiang, W. Synthetic Biology Approaches for Chromosomal Integration of Genes and Pathways in Industrial Microbial Systems.

Biotechnol. Adv. **2019**, *37* , 730–745. https://doi.org/10.1016/j.biotechadv.2019.04.002.

(12) Ferreira, J. A.; Mahboubi, A.; Lennartsson, P. R.; Taherzadeh, M. J. Waste Biorefineries Using Filamentous Ascomycetes Fungi: Present Status and Future Prospects. *Bioresour. Technol.* **2016**, *215*, 334–345. https://doi.org/10.1016/j.biortech.2016.03.018.

(13) Nayak, T.; Szewczyk, E.; Oakley, C. E.; Osmani, A.; Ukil, L.; Murray, S. L.; Hynes, M. J.; Osmani, S. A.; Oakley, B. R. A Versatile and Efficient Gene-Targeting System for *Aspergillus nidulans*. *Genetics* **2006**, *172*, 1557–1566. https://doi.org/10.1534/genetics.105.052563.

(14) Nielsen, M. T.; Nielsen, J. B.; Anyaogu, D. C.; Holm, D. K.; Nielsen, K. F.; Larsen, T. O.; Mortensen, U. H. Heterologous Reconstitution of the Intact Geodin Gene Cluster in *Aspergillus nidulans* through a Simple and Versatile PCR Based Approach. *PLoS One* **2013**, *8* , e72871. https://doi.org/10.1371/journal.pone.0072871.

(15) Yin, W. B.; Chooi, Y. H.; Smith, A. R.; Cacho, R. A.; Hu, Y.; White, T. C.; Tang, Y. Discovery of Cryptic Polyketide Metabolites from Dermatophytes Using Heterologous Expression in *Aspergillus nidulans*. *ACS Synth. Biol.* **2013**, *2*, 629–634. https://doi.org/10.1021/sb400048b.

(16) Robey, M. T.; Caesar, L. K.; Drott, M. T.; Keller, N. P.; Kelleher, N. L. An Interpreted Atlas of Biosynthetic Gene Clusters from 1,000 Fungal Genomes. *Proc. Natl. Acad. Sci.* **2021**, *118*, e2020230118. https://doi.org/10.1073/pnas.2020230118.

(17) Olorunniji, F. J.; Rosser, S. J.; Stark, W. M. Site-Specific Recombinases: Molecular Machines for the Genetic Revolution. *Biochem. J.* **2016**, *473*, 673–684. https://doi.org/10.1042/BJ20151112.

(18) Hirano, N.; Muroi, T.; Takahashi, H.; Haruki, M. Site-Specific Recombinases as Tools for Heterologous Gene Integration. *Appl. Microbiol. Biotechnol.* **2011**, *92*, 227–239. https://doi.org/10.1007/s00253-011-3519-5.

(19) Santos, C. N. S.; Regitsky, D. D.; Yoshikuni, Y. Implementation of Stable and Complex Biological Systems through Recombinase-Assisted Genome Engineering. *Nat. Commun.* **2013**, *4*, 2503. https://doi.org/10.1038/ncomms3503.

(20) Wallace, H. A. C.; Marques-Kranc, F.; Richardson, M.; Luna-Crespo, F.; Sharpe, J. A.; Hughes, J.; Wood, W. G.; Higgs, D. R.; Smith, A. J. H. Manipulating the Mouse Genome to Engineer Precise Functional Syntenic Replacements with Human Sequence. *Cell* **2007**, *128*, 197–209. https://doi.org/10.1016/j.cell.2006.11.044.

(21) Wang, G.; Zhao, Z.; Ke, J.; Engel, Y.; Shi, Y.-M.; Robinson, D.; Bingol, K.; Zhang, Z.; Bowen, B.; Louie, K.; Wang, B.; Evans, R.; Miyamoto, Y.; Cheng, K.; Kosina, S.; De Raad, M.; Silva, L.; Luhrs, A.; Lubbe, A.; Hoyt, D. W.; Francavilla, C.; Otani, H.; Deutsch, S.; Washton, N. M.; Rubin, E. M.; Mouncey, N. J.; Visel, A.; Northen, T.; Cheng, J.-F.; Bode, H. B.; Yoshikuni, Y. CRAGE Enables Rapid Activation of Biosynthetic Gene Clusters in Undomesticated Bacteria. *Nat. Microbiol.* **2019**, *4*, 2498–2510. https://doi.org/10.1038/s41564-019-0573-8.

(22) Garcia-Morales, L.; Ruiz, E.; Gourgues, G.; Rideau, F.; Piñero-Lambea, C.; Lluch-Senar, M.; Blanchard, A.; Lartigue, C. A RAGE Based Strategy for the Genome Engineering of the Human Respiratory Pathogen *Mycoplasma pneumoniae*. *ACS Synth. Biol.* **2020**, *9*, 2737–2748. https://doi.org/10.1021/acssynbio.0c00263.

(23) Baer, A.; Bode, J. Coping with Kinetic and Thermodynamic Barriers: RMCE, an Efficient Strategy for the Targeted Integration of Transgenes. *Curr. Opin. Biotechnol.* **2001**, *12*, 473–480. https://doi.org/10.1016/S0958-1669(00)00248-2.

(24) Forment, J. V.; Ramón, D.; MacCabe, A. P. Consecutive Gene Deletions in *Aspergillus nidulans*: Application of the Cre/*loxP* System. *Curr. Genet.* **2006**, *50*, 217–224. https://doi.org/10.1007/s00294-006-0081-2.

(25) Krappmann, S.; Bayram, Ö.¨; Braus, G. H. Deletion and Allelic Exchange of the *Aspergillus fumigatus veA* Locus via a Novel Recyclable Marker Module. *Eukaryot. Cell* **2005**, *4* , 1298–1307. https://doi.org/10.1128/EC.4.7.1298-1307.2005.

(26) Mizutani, O.; Masaki, K.; Gomi, K.; Iefuji, H. Modified Cre-loxP Recombination in *Aspergillus oryzae* by Direct Introduction of Cre Recombinase for Marker Gene Rescue. *Appl. Environ. Microbiol.* **2012**, *78*, 4126–4133. https://doi.org/10.1128/AEM.00080-12.

(27) Steiger, M. G.; Vitikainen, M.; Uskonen, P.; Brunner, K.; Adam, G.; Pakula, T.; Penttilä, M.; Saloheimo, M.; MacH, R. L.; Mach-Aigner, A. R. Transformation System for *Hypocrea Jecorina* (*Trichoderma Reesei*) That Favors Homologous Integration and Employs Reusable Bidirectionally Selectable Markers. *Appl. Environ. Microbiol.* **2011**, *77*, 114–121. https://doi.org/10.1128/AEM.02100-10.

(28) Honda, S.; Selker, E. U. Tools for Fungal Proteomics: Multifunctional *Neurospora* Vectors for Gene Replacement, Protein Expression and Protein Purification. *Genetics* **2009**, *182*, 11–23. https://doi.org/10.1534/genetics.108.098707.

(29) Florea, S.; Andreeva, K.; Machado, C.; Mirabito, P. M.; Schardl, C. L. Elimination of Marker Genes from Transformed Filamentous Fungi by Unselected Transient

Transfection with a Cre-Expressing Plasmid. *Fungal Genet. Biol.* **2009**, *46* , 721–730. https://doi.org/10.1016/j.fgb.2009.06.010.

(30) Jiang, B.; Zhang, R.; Feng, D.; Wang, F.; Liu, K.; Jiang, Y.; Niu, K.; Yuan, Q.; Wang, M.; Wang, H.; Zhang, Y.; Fang, X. A Tet-on and Cre-*loxP* Based Genetic Engineering System for Convenient Recycling of Selection Markers in *Penicillium oxalicum*. *Front. Microbiol.* **2016**, *7* , 485. https://doi.org/10.3389/fmicb.2016.00485.

(31) Krappmann, S. Genetic Surgery in Fungi: Employing Site-Specific Recombinases for Genome Manipulation. *Appl. Microbiol. Biotechnol.* **2014**, *98*, 1971–1982. https://doi.org/10.1007/s00253-013-5480-y.

(32) Lee, G.; Saito, I. Role of Nucleotide Sequences of *loxP* Spacer Region in Cre-Mediated Recombination. *Gene* **1998**, *216*, 55–65. https://doi.org/10.1016/S0378-1119(98)00325-4.

(33) Albert, H.; Dale, E. C.; Lee, E.; Ow, D. W. Site-specific Integration of DNA into Wild-type and Mutant *lox* Sites Placed in the Plant Genome. *Plant J.* **1995**, *7* , 649–659. https://doi.org/10.1046/j.1365-313X.1995.7040649.x.

(34) Chiang, Y. M.; Ahuja, M.; Oakley, C. E.; Entwistle, R.; Asokan, A.; Zutz, C.; Wang, C. C. C.; Oakley, B. R. Development of Genetic Dereplication Strains in *Aspergillus nidulans* Results in the Discovery of Aspercryptin. *Angew. Chemie - Int. Ed.* **2016**, *55*, 1662–1665. https://doi.org/10.1002/anie.201507097.

(35) Roux, I.; Woodcraft, C.; Hu, J.; Wolters, R.; Gilchrist, C. L. M.; Chooi, Y. H. CRISPR-Mediated Activation of Biosynthetic Gene Clusters for Bioactive Molecule Discovery in Filamentous Fungi. *ACS Synth. Biol.* **2020**, *9*, 1843–1854. https://doi.org/10.1021/acssynbio.0c00197.

(36) Gilchrist, C. L. M.; Lacey, H. J.; Vuong, D.; Pitt, J. I.; Lange, L.; Lacey, E.; Pilgaard, B.; Chooi, Y. H.; Piggott, A. M. Comprehensive Chemotaxonomic and Genomic Profiling of a Biosynthetically Talented Australian Fungus, *Aspergillus burnettii* Sp. Nov. *Fungal Genet. Biol.* **2020**, *143*, 103435. https://doi.org/10.1016/j.fgb.2020.103435.

(37) Jensen, N. B.; Strucko, T.; Kildegaard, K. R.; David, F.; Maury, J.; Mortensen, U. H.; Forster, J.; Nielsen, J.; Borodina, I. EasyClone: Method for Iterative Chromosomal Integration of Multiple Genes in *Saccharomyces cerevisiae*. *FEMS Yeast Res.* **2014**, *14* , 238–248. https://doi.org/10.1111/1567-1364.12118.

(38) Vanegas, K. G.; Jarczynska, Z. D.; Strucko, T.; Mortensen, U. H. Cpf1 Enables Fast and Efficient Genome Editing in *Aspergilli*. *Fungal Biol. Biotechnol.* **2019**, *6* , 6.

https://doi.org/10.1186/s40694-019-0069-6.

(39) Robellet, X.; Oestreicher, N.; Guitton, A.; Vélot, C. Gene Silencing of Transgenes Inserted in the *Aspergillus nidulans alcM* And/or *alcS Loci*. *Curr. Genet.* **2010**, *56* , 341–348. https://doi.org/10.1007/s00294-010-0303-5.

(40) Van Leeuwe, T. M.; Arentshorst, M.; Ernst, T.; Alazi, E.; Punt, P. J.; Ram, A. F. J. Efficient Marker Free CRISPR/Cas9 Genome Editing for Functional Analysis of Gene Families in Filamentous Fungi. *Fungal Biol. Biotechnol.* **2019**, *6*, 13. https://doi.org/10.1186/s40694-019-0076-7.

(41) Jarczynska, Z. D.; Rendsvig, J. K. H.; Pagels, N.; Viana, V. R.; Nødvig, C. S.; Kirchner, F. H.; Strucko, T.; Nielsen, M. L.; Mortensen, U. H. DIVERSIFY – a Fungal Multi-Species Gene Expression Platform. *ACS Synth. Biol.* **2020**. https://doi.org/10.1021/acssynbio.0c00587.

(42) Axelrod, D. E.; Gealt, M.; Pastushok, M. Gene Control of Developmental Competence in *Aspergillus nidulans*. *Dev. Biol.* **1973**, *34* , 9–15. https://doi.org/10.1016/0012-1606(73)90335-7.

(43) Adams, T. H.; Wieser, J. K.; Yu, J.-H. Asexual Sporulation in *Aspergillus nidulans*. *Microbiol. Mol. Biol. Rev.* **1998**, *62* , 545–545. https://doi.org/10.1128/mmbr.62.2.545-545.1998.

(44) Wang, F.; Sethiya, P.; Hu, X.; Guo, S.; Chen, Y.; Li, A.; Tan, K.; Wong, K. H. Transcription in Fungal Conidia before Dormancy Produces Phenotypically Variable Conidia That Maximize Survival in Different Environments. *Nat. Microbiol.* **2021**, *6*, 1066–1081. https://doi.org/10.1038/s41564-021-00922-y.

(45) Sarkari, P.; Marx, H.; Blumhoff, M. L.; Mattanovich, D.; Sauer, M.; Steiger, M. G. An Efficient Tool for Metabolic Pathway Construction and Gene Integration for *Aspergillus niger*. *Bioresour. Technol.* **2017**, *245*, 1327–1333. https://doi.org/10.1016/j.biortech.2017.05.004.

(46) De Lorenzo, V.; Krasnogor, N.; Schmidt, M. For the Sake of the Bioeconomy : Define What a Synthetic Biology Chassis Is ! *N. Biotechnol.* **2021**, *60*, 44–51. https://doi.org/10.1016/j.nbt.2020.08.004.

(47) Pall, M. L.; Brunelli, J. P. A Series of Six Compact Fungal Transformation Vectors Containing Polylinkers with Multiple Unique Restriction Sites. *Fungal Genet. Rep.* **1993**, *40* , 59–62. https://doi.org/10.4148/1941-4765.1413.

(48) Fang, F.; Salmon, K.; Shen, M. W. Y.; Aeling, K. A.; Ito, E.; Irwin, B.; Tran, U. P. C.;

Hatfield, G. W.; Da Silva, N. A.; Sandmeyer, S. A Vector Set for Systematic Metabolic Engineering in *Saccharomyces cerevisiae*. *Yeast* **2011**, *28*, 123–136. https://doi.org/10.1002/yea.1824.

(49) Chooi, Y. H.; Fang, J.; Liu, H.; Filler, S. G.; Wang, P.; Tang, Y. Genome Mining of a Prenylated and Immunosuppressive Polyketide from Pathogenic Fungi. *Org. Lett.* **2013**, *15* (4), 780–783. https://doi.org/10.1021/ol303435y.

(50) Tsunematsu, Y.; Ishikawa, N.; Wakana, D.; Goda, Y.; Noguchi, H.; Moriya, H.; Hotta, K.; Watanabe, K. Distinct Mechanisms for Spiro-Carbon Formation Reveal Biosynthetic Pathway Crosstalk. *Nat. Chem. Biol.* **2013**, *9*, 818–825. https://doi.org/10.1038/nchembio.1366.

(51) Boyce, K. J.; Bugeja, H. E.; Weerasinghe, H.; Payne, M. J.; Schreider, L. Strategies for the Molecular Genetic Manipulation and Visualization of the Human Fungal Pathogen *Penicillium marneffei*. *Fungal Genet. Rep.* **2012**, *59*, 1–12. https://doi.org/10.4148/1941-4765.1009.

(52) Lim, F. Y.; Sanchez, J. F.; Wang, C. C. C.; Keller, N. P. Toward Awakening Cryptic Secondary Metabolite Gene Clusters in Filamentous Fungi. *Methods Enzymol.* **2012**, *517*, 303–324. https://doi.org/10.1016/B978-0-12-404634-4.00015-2.

(53) Chooi, Y. H.; Zhang, G.; Hu, J.; Muria-Gonzalez, M. J.; Tran, P. N.; Pettitt, A.; Maier, A. G.; Barrow, R. A.; Solomon, P. S. Functional Genomics-Guided Discovery of a Light- Activated Phytotoxin in the Wheat Pathogen *Parastagonospora nodorum* via Pathway Activation. *Environ. Microbiol.* **2017**, *19*, 1975–1986. https://doi.org/10.1111/1462-2920.13711.

Supplementary Information

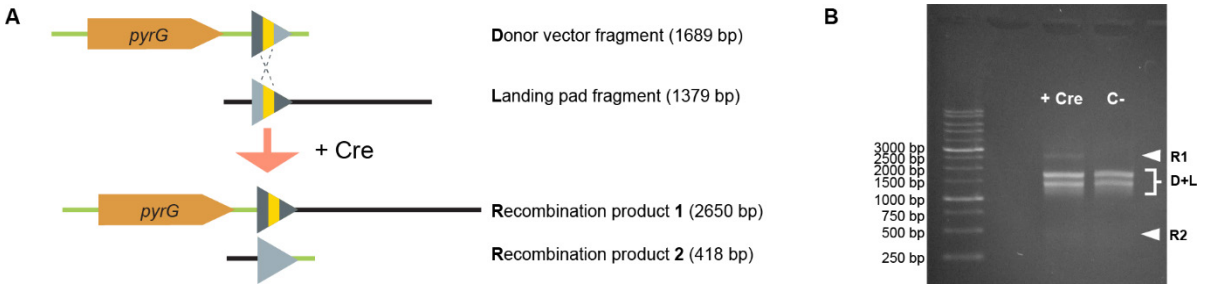

Figure S1 Validation of the double mutant site *lox2272-66/71*. **A.** Experimental set up. Fragments were amplified by PCR containing the site *lox2272-66* or *lox2272-72*. After *in vitro* recombination mediated by Cre, two recombination products are formed of different length compared to the substrates of recombination. **B.** Gel electrophoresis run after *in vitro* recombination reveals a new band of the size of recombination product 1 in the sample treated with Cre recombinase compared to the control. Recombination product 2 is less evident due to its smaller size and mass. According to the instructions from the manufacturer (NEB), the efficiency of *in vitro* Cre recombination is low for which this assay is a qualitative approximation. Nevertheless, a new band of the expected size of the bigger recombination product was observed validating the designed *lox2272-66/71* pair.

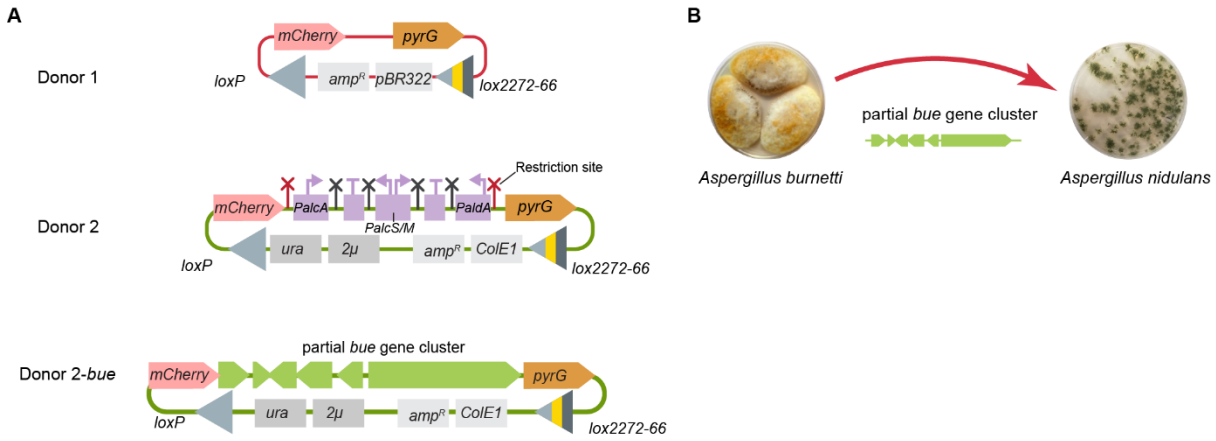

Figure S2 Donor vectors evaluated for RMCE-LE/RE. **A.** Donor vector 1 is a small 6.6 kb vector used in initial testing. Donor 2 is a 12.3 kb shuttle vector with components for replication and selection on *Saccharomyces cerevisiae* (*ura*, *2μ*) and *E. coli* (*ampR*, *ColE1*). Donor 2 contains four alcohol inducible promoters for heterologous expression derived from the vector pYFAC-CH2 [1], and it also allows excising the multiple promoter cassette and cloning large gene fragments under native promoters by digesting with EcoRI (red restriction sites). As an example, we cloned an 18 kb region of *Aspergillus burnetti* containing genes from the *bue* BGC, resulting in a 27.3 kb vector. **B.** Overview of proof-of-concept integration of a fragment from the *bue* biosynthetic gene cluster from *A. burnetti* in *A nidulans*.

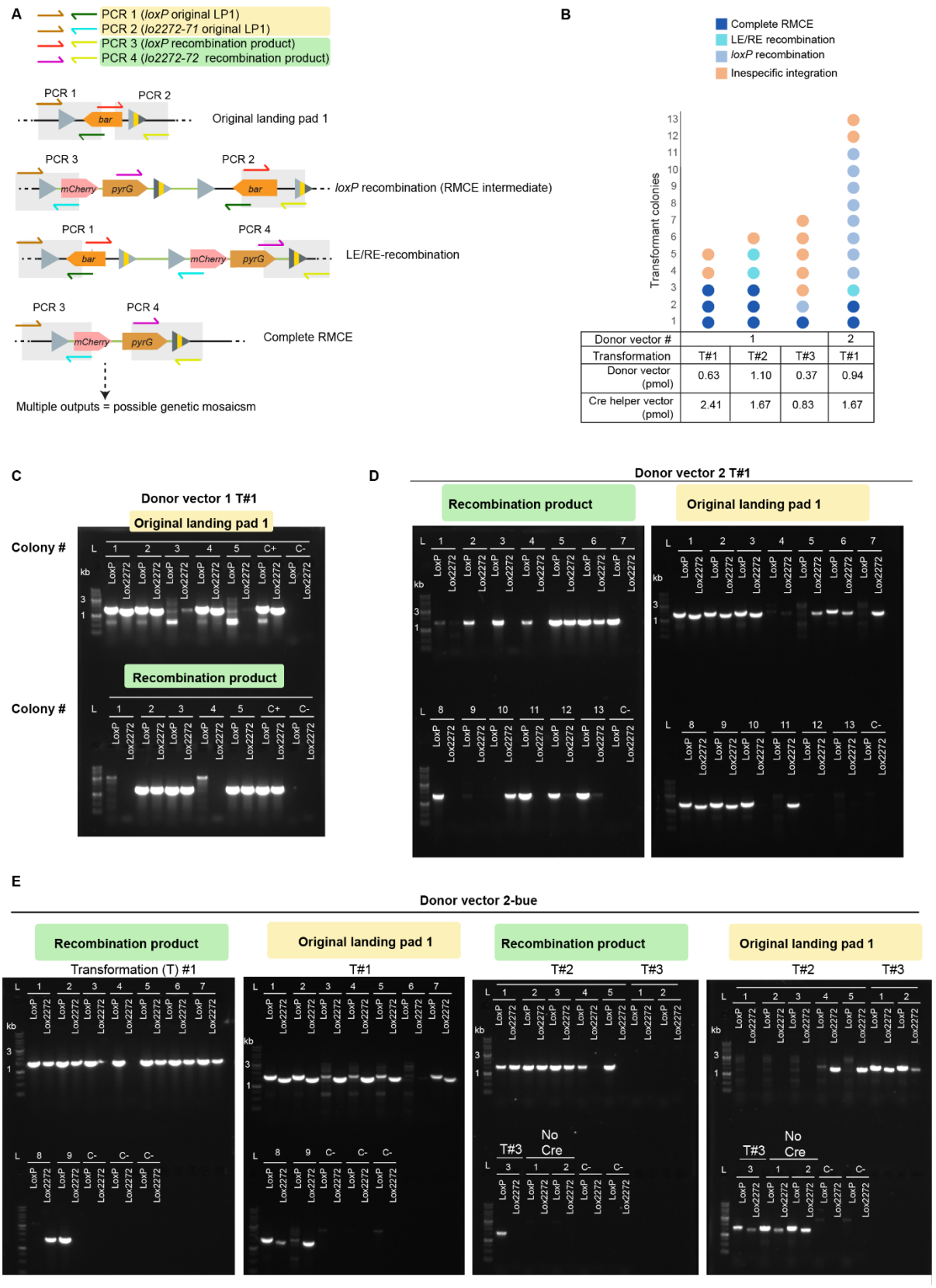

Figure S3 PCR-based screening of recombinant colonies. **A.** Overview of the PCR screening strategy. gDNA from each transformant colony is analysed by four PCR to determine the possible recombination outputs. **B.** Amount of transformant colonies obtained in different

transformation experiments with Donor vector 1 (6.6 kb) and Donor vector 2 (12.2 kb), with the integration mechanism indicated as a colour code, as analysed by PCR. Recombination is obtained across a different amount and proportion of donor vector and Cre helper vector. Recombination is observed with both donor vector 1 and donor 2. **C.** Representative gel of the PCR results of a transformation event with donor vector 1, different transformant colonies are indicated as numbers. **D.** Representative gel of the PCR results of a transformation event with donor vector 2, different transformant colonies are indicated as numbers. **E.** PCR results of a transformation events with donor vector 2-bue (27.7 kb vector, 21 kb floxed insert), different transformant colonies are indicated as numbers.

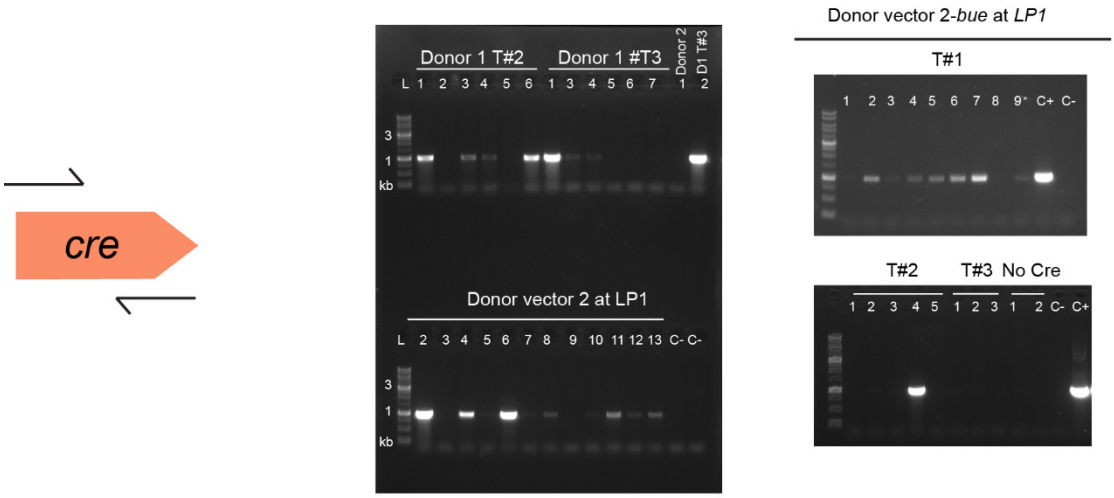

Figure S4 Screening for presence of *cre* expression cassette. PCR positive results are found in several transformant colonies with high variability across experiments (0% – 60% colonies per transformation event).These results seem could imply that random integration of the *cre* helper vector might occur in *Aspergillus nidulans* or that traces of the residual vector might be present at later growth stages.

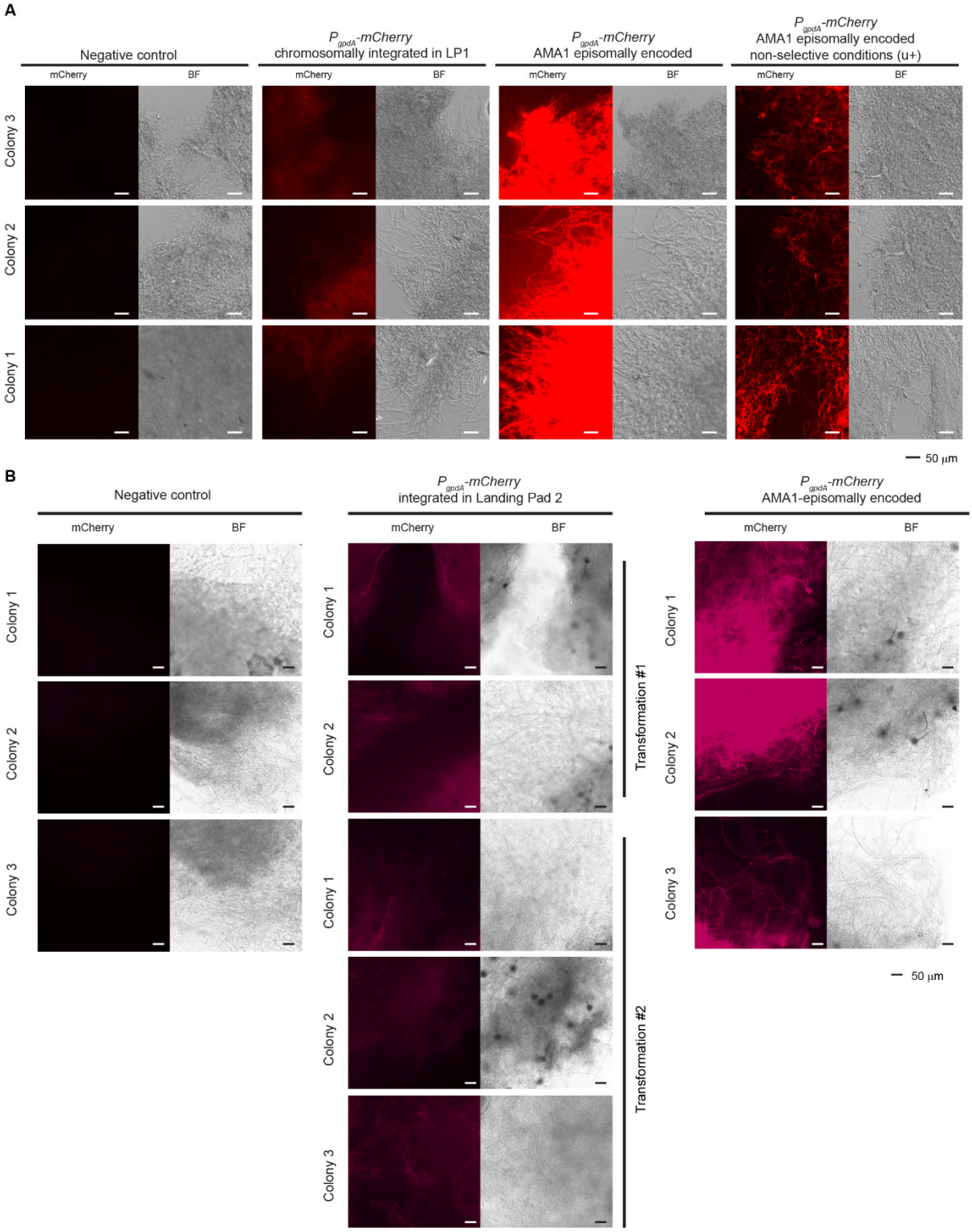

Figure S5. *P_{gpdA}-mCherry* expression from chromosomal and episomal contexts observed in mycelia. **A.** Strains with *P_{gpdA}-mCherry* integrated at LP1 show low *mCherry* expression in mycelia, but distinguishable from the negative control. Expression at LP1 is lower than episomal expression when growing on selective media (lacking uracil and uridine). AMA1-based episomal expression in mycelia grown under non-selective conditions (supplemented uracil and uridine) shows a sparce pattern, but some hyphae still shows higher signal than

strains with chromosomal expression at LP1. The spores for each sample were collected from three individual colonies representing biological replicates of a recombinant strain and grown overnight in liquid stationary culture at 37 °C. **B.** Integration of the donor vector 2-*bue* at LP2 results in low mCherry expression in mycelia, but distinguishable from the negative control. Expression at LP2 is lower than episomal expression under selective conditions. All samples were grown on selective media unless specified otherwise. The spores from each sample were collected from individual transformant colonies, and different transformation events when indicated, and grown overnight in liquid stationary culture at 37 °C. Samples with similar mycelial growth were observed under mCherry filter and brightfield (BF). Scale bar 50 µm.

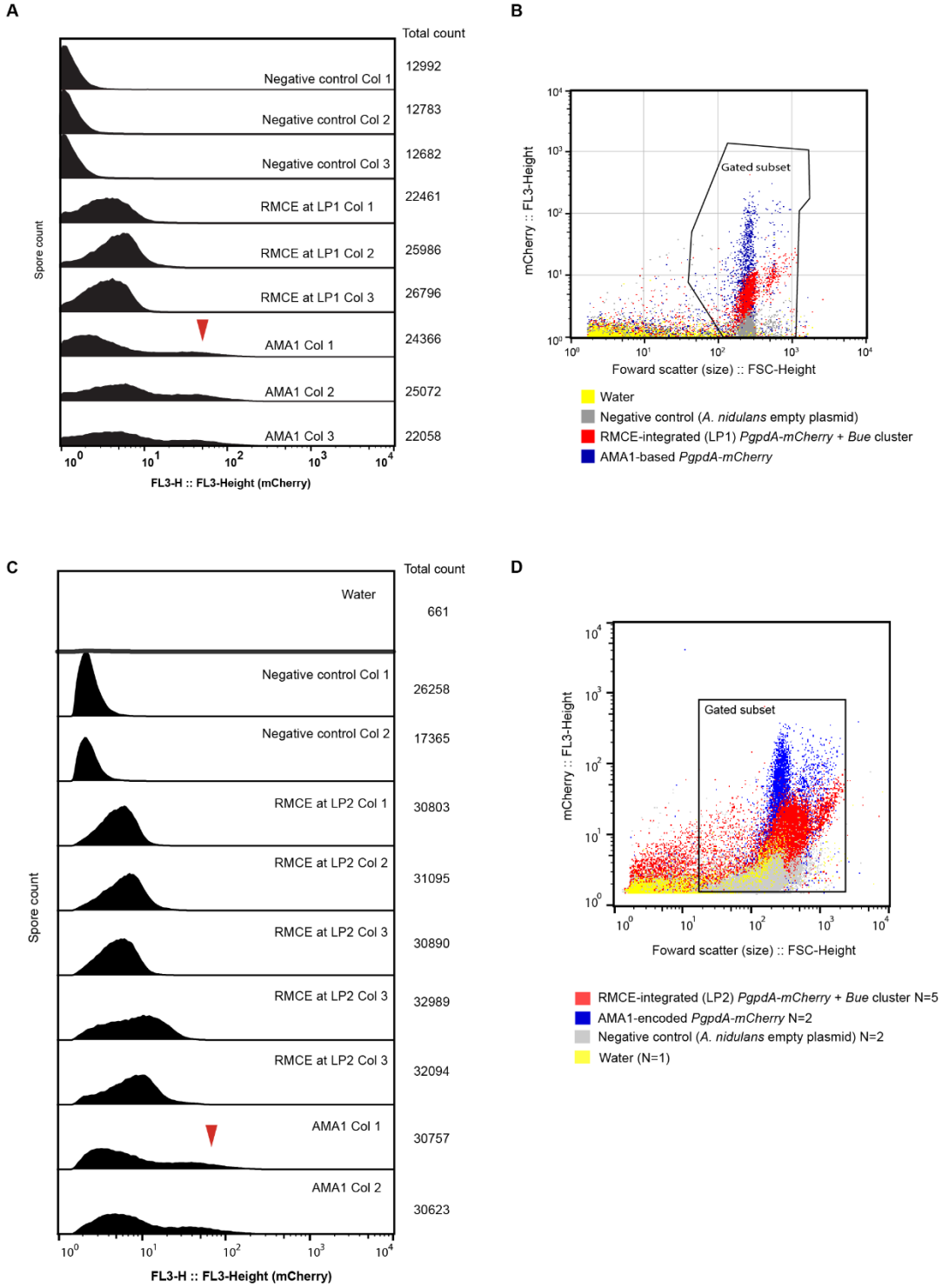

Figure S6 Analysis of mCherry in spores by flow cytometry with biological replicates. **A.** Analysis of expression at LP1. Histograms show spore count vs FL3-Height which is indicative of mCherry signal. We observe that the samples with *PgpdA-mCherry* integrated at LP1 show fluorescence distinguishable to the negative control, and a more compact distribution than AMA1-based expression. However, a proportion of the spores from colonies with AMA1-based vectors can reach fluorescence levels one order of magnitude higher than spores with

chromosomal expression at LP1 (see red arrow). Gated event count numbers are indicated at the right. **B.** Ungated plots showing the total of events and gating strategy for analysis at LP1. **C.** Analysis of expression at LP2. Histograms show spore count vs FL3-Height which is indicative of mCherry signal. We observe higher signal in the strains with chromosomal integrated mCherry than the control *A. nidulans* strain (empty plasmid). However, signal at LP2 (IS1) is also lower than the higher range of signal from AMA1-based mCherry expression (red arrow). **D.** Ungated plots showing the total events, *y* axis represent mCherry signal and x axis represents particle size. Gating strategy is indicated.

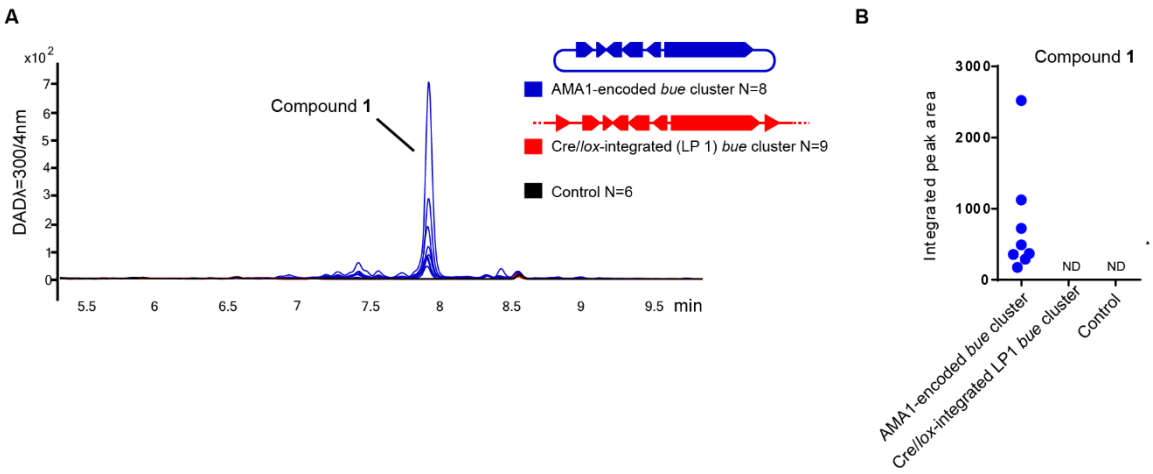

Figure S7. Evaluation of compound production. **A.** DAD (λ=300 nm) chromatograms of culture media extracts of *A. nidulans* encoding the genes *bueA/B/C/D/E/R* on AMA1 episomal vectors show production of compound **1**, unlike the strains where *bueA/B/C/D/E/R* are chromosomally integrated at LP1 and in the negative control. **B.** Integrated peak area of the chromatogram in the left, showing the variability in compound production between strains.

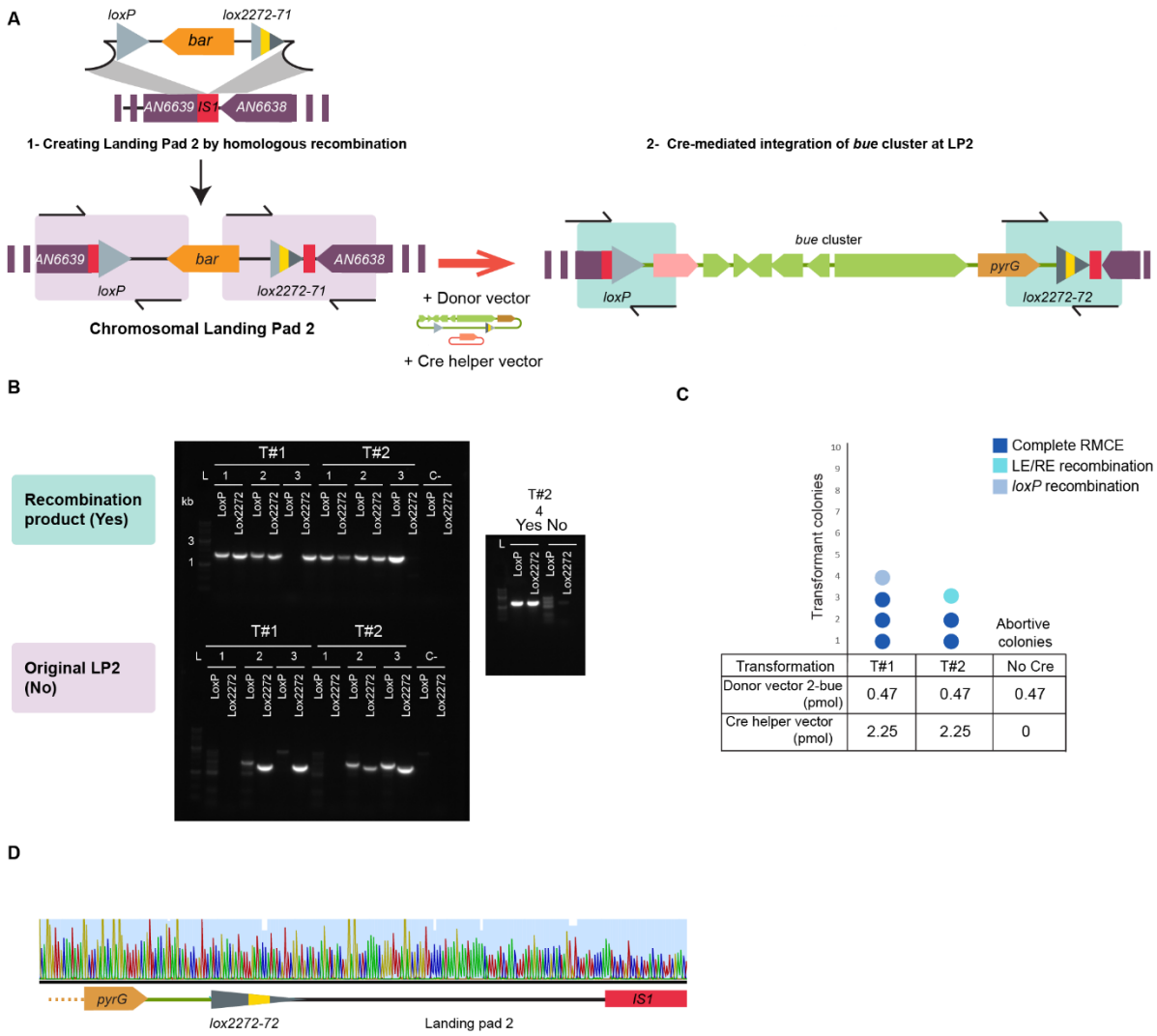

Figure S7. Evaluation of integration of donor vector 2-bue at LP2. **A.** Schematic overview of the experimental setup to build and test LP2**. B.** PCR screening results of two different transformation events with donor vector 2-bue, different transformant colonies are indicated as numbers. **C.** Number of transformant colonies obtained in different transformation experiments, with the integration mechanism indicated as a colour code, as analysed by PCR. **D.** Sanger sequencing of representative PCR amplicon, confirming the site *lox2272-72* after recombination at LP2.

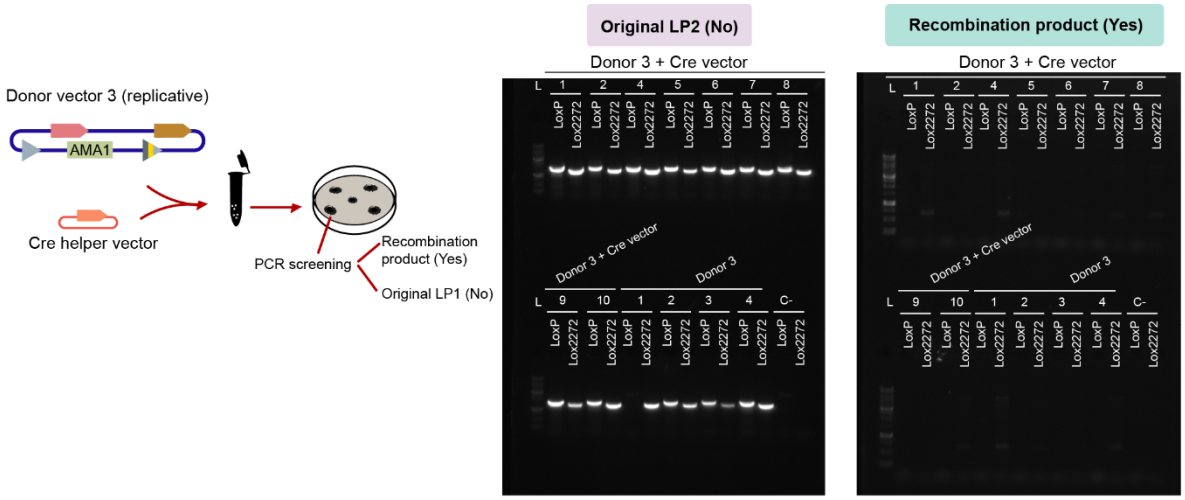

Figure S8 Evaluation of a replicative AMA1-based donor-vector. Overview of the experimental setup (Left). PCR screening indicates that selecting for AMA1-vector uptake is not sufficient to obtaining recombinant colonies, and strategies to select the recombination event might be needed.

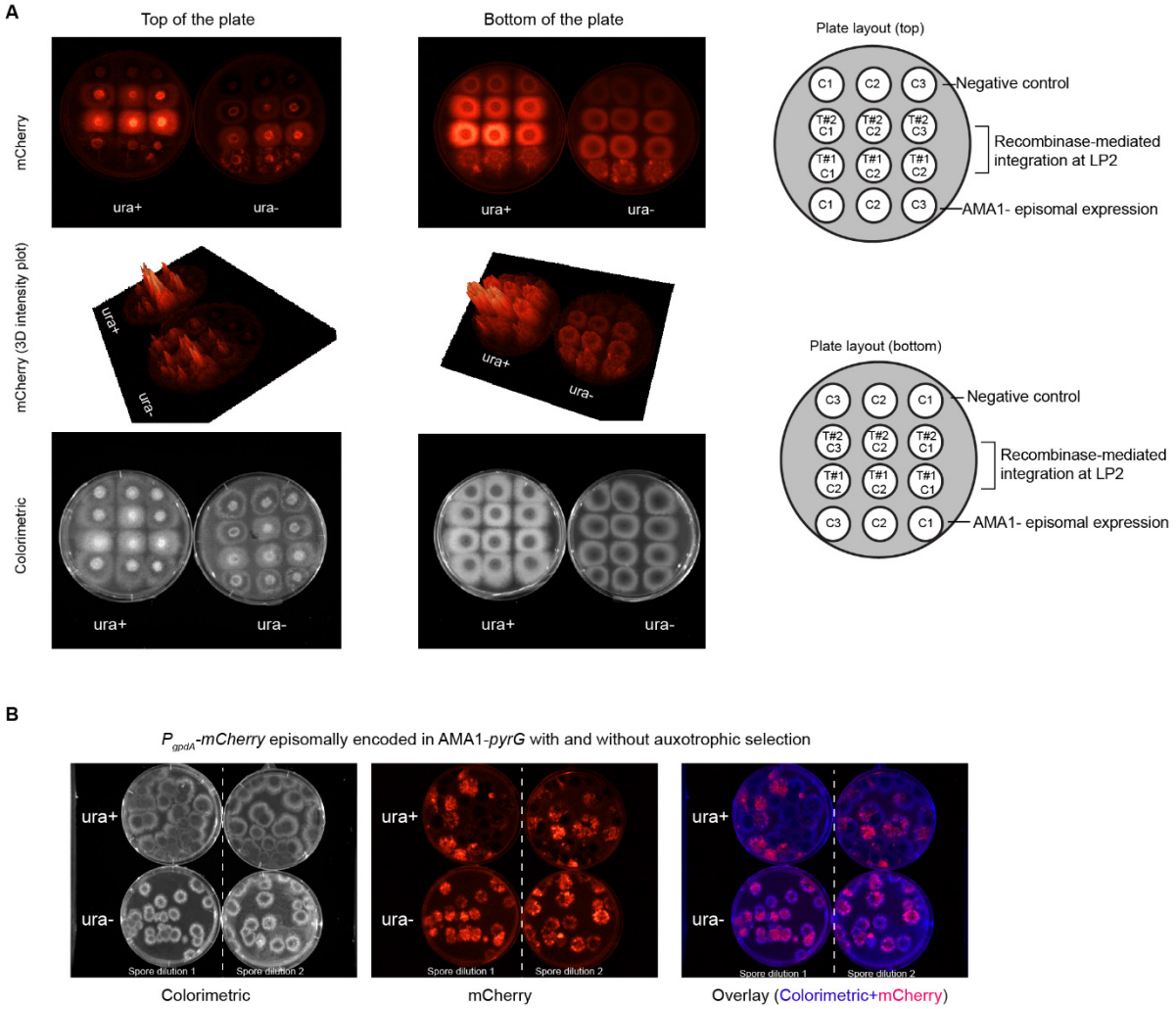

Figure S9 Visual inspection of fluorescent phenotype of integrative and episomal P_{gpdA}-*mCherry* in *A. nidulans* colonies. **A.** Colonies growing under non-selective (ura+) and selective (ura-) conditions. Images were acquired from both the bottom and the top of the plate. Plate layouts are shown on the right indicating the transformation event and the colony number. Images taken with green light for excitation an mCherry filter show uniform fluorescence in the strains with P_{gpdA}-*mCherry* chromosomally integrated, compared to the controls. The strains with episomal AMA1-encoded P_{gpdA}-*mCherry* show a patchy pattern of fluorescence. The mCherry signal 3D intensity plot is included to aid the interpretation of mCherry signal. The colorimetric images (white light) are on the bottom. Plates were incubated at 37 °C for three days. **B.** Difference in genetic stability and fluorescence pattern observed in *A. nidulans* colonies product of plating a spore dilution containing AMA1-pyrG encoded P_{gpdA}-*mCherry*. As each colony arises from an individual spore, we can observe that under selective conditions all colonies retain fluorescence. Under non-selective conditions, many of the colonies do not show fluorescence. Interestingly, many of the fluorescent colonies under non-selective conditions demonstrate fluorescence comparable to the colonies under selection condition. We also observe more colonies in the plates with no selection pressure (~30 colonies) than in

the plates with selection pressure (21-25 colonies) , which is indicative of the genetic stability of AMA1-pyrG. Plates were incubated at 37 °C for three days.

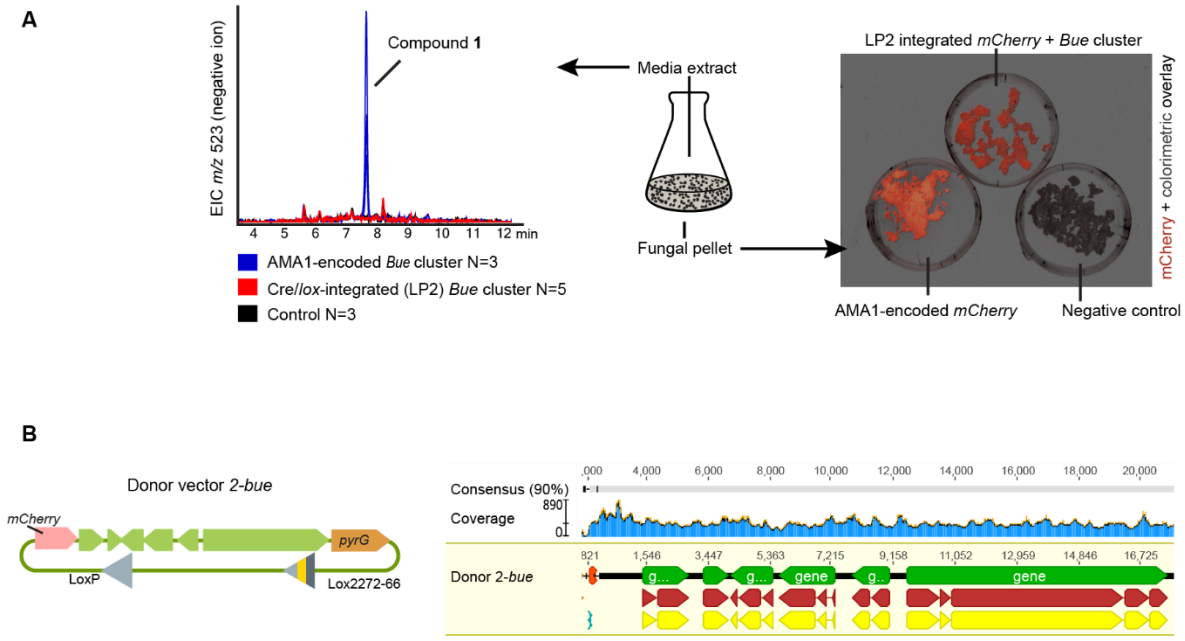

Figure S10 Chromosomal integration at LP2 does not result in detectable production of compound **1**. **A.** (Left) Extracted ion chromatogram on negative ion mode for *m/z* 523 ± 0.5 shows a peak in the strains with AMA1-encoded bue cluster genes (blue) but not in the strains with chromosomally integrated bue cluster genes (red) or the control (black). (Right) Fungal pellets from the end of the culturing period were filtered an observed by fluorescence photography. Fluorescence was observed in the strains with AMA1-encoded P_{gpdA}-*mCherry* and strains with P_{gpdA}-*mCherry* chromosomally integrated at LP2. **B.** The plasmid Donor2-bue was analysed with whole plasmid-sequencing for troubleshooting the lack of compound production. No mutations were observed, with all the bue cluster cloned region having coverage of ≥110 and a consensus of ≥90%.

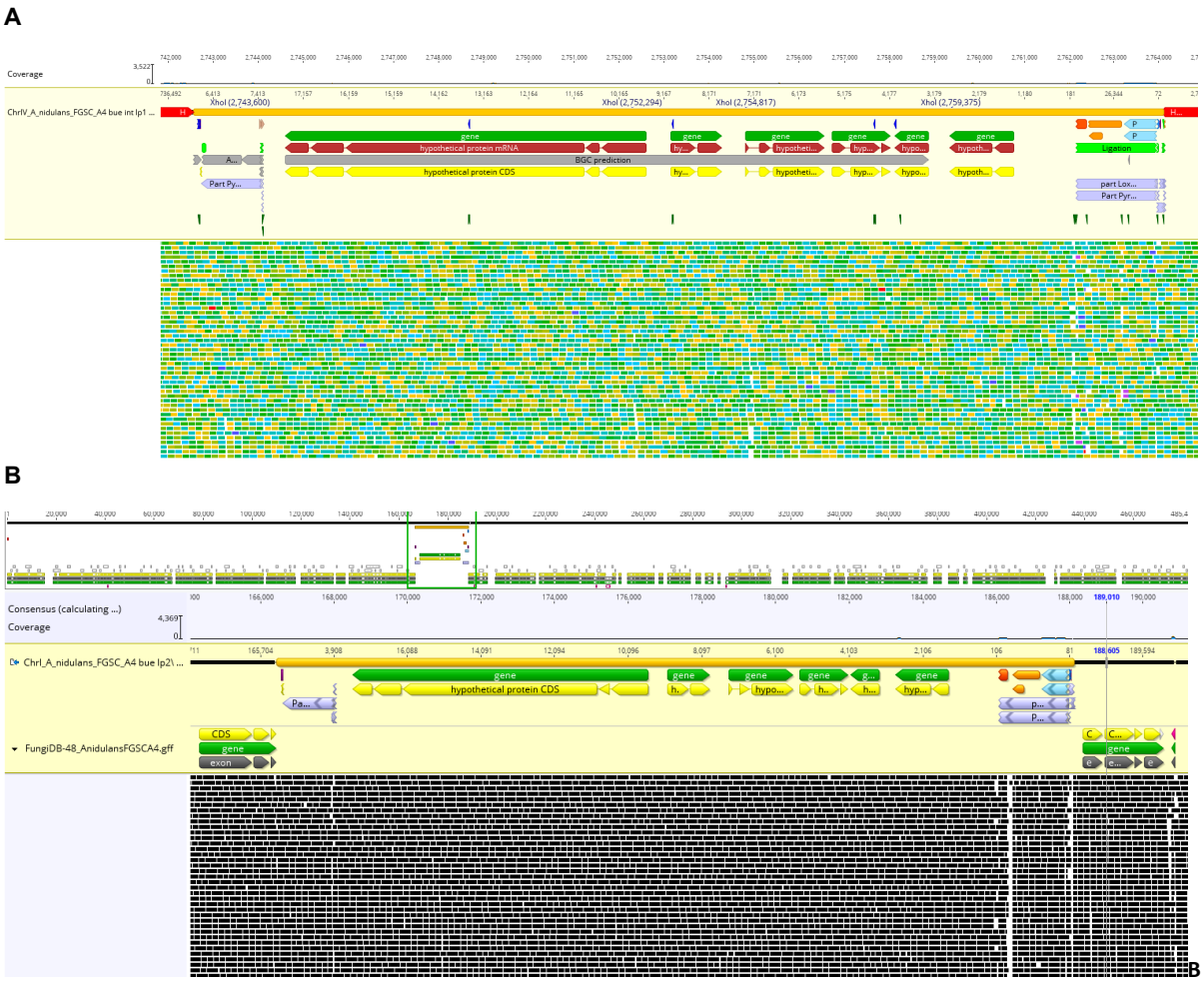

Figure S11 Chromosomal integration of *bue* genes at LP1 (**A**) and LP2 (**B**) observed by whole genome sequencing. Biological duplicate from with *bue* genes integrated at LP2 (biological duplicates) also demonstrate de expected recombination event and no mutations on *bue* genes that could explain the lack of compound production from a chromosomal context. Low quality alignments on the right region of the figure are caused by the presence of *A. nidulans* P_{gpdA} and T_{trpC} in *mCherry* expression cassette. Figure visualised in Geneious 11.03.

Table S1 DNA sequence of *lox* recombination sites used, 5′ to 3′. The nucleotides that differ from the wt *loxP* sequence are underlined. The symbol used for each lox site is indicated at the right column.

Site	Arm	Core	Arm	Symbol
loxP	ATAACTTCGTATA	ATGTATGC	TATACGAAGTTAT	
lox2272-71	ATAACTTCGTATA	A<u>A</u>GTAT<u>C</u>C	TATACGAA<u>CGGTA</u>	
lox2272-66	<u>TACCG</u>TTCGTATA	A<u>A</u>GTAT<u>C</u>C	TATACGAAGTTAT	
lox2272-72	<u>TACCG</u>TTCGTATA	A<u>A</u>GTAT<u>C</u>C	TATACGAA<u>CGGTA</u>	
lox2272	ATAACTTCGTATA	A<u>A</u>GTAT<u>C</u>C	TATACGAAGTTAT	

Table S2 Vectors used in this work.

Vector name	Purpose and name in the text	Origin	Addgene ID
pGem-PgpdA-Cre-TtrpC	Helper vector for the expression of Cre. Not replicative on *A. nidulans*.	This work	168784
pGemLP1-loxP-bar-Lox2272-71	Vector to create LP1 by homologous recombination.	This work	168785
pGemLP2-loxP-bar-Lox2272-71	Vector to create LP2 by homologous recombination.		168786
pGem-loxp-mcherry-lox66-2272	Donor vector 1	This work	-
pRecomb-loxp-mcherry-4Gcloningsite-lox66-2272	Donor vector 2	This work	-
pRecomb-loxp-mcherry-bueABCDER-lox66-2272	Donor vector 2-bue	This work	168787
pKW20088-loxP-mcherry-pyrG-lox66-227266	Donor vector 3	This work	-
pYFAC-bueABCDER	AMA1-based expression of bueA/B/C/D/E/R (*pyrG* marker).	Unpublished	
pYFAC-bueG-PgpdA-bueR	Transcription factor overexpression for *bue* cluster activation (*pyroA* marker).	Unpublished	

Table S3 Genotype of parental strains used in this work.

Parental strains	Relevant genotype
A. nidulans LO8030 [2]	pyroA4, riboB2, pyrG89, nkuA::argB, Sterigmatocystin cluster (AN7804-AN7825)Δ, emericellamide cluster (AN2545-AN2549)Δ, asperfuranone cluster (AN1039-AN1029)Δ, monodictyphenone cluster (AN10023-AN10021)Δ, terraquinone cluster (AN8512-AN8520)Δ, austinol cluster part1 (AN8379-AN8384)Δ, austinol cluster part2 (AN9246-AND9259)Δ, f9775 (AN7906-AN7915)Δ, asperthecin cluster (AN6000-AN60002)Δ
LO8030-LP1	LO8030 + loxP-bar-lox2272-71::Sterigmatocystin cluster (AN7804-AN7825)Δ
LO8030-LP2	LO8030 + loxP-bar-lox2272-71::IS1
LO8030-LP1-bueA/B/C/D/E/R	LO8030 + loxP-mCherry-bueA/B/C/D/E/R-pyrG-lox2272-72::Sterigmatocystin cluster (AN7804-AN7825)Δ
LO8030-LP2-bueA/B/C/D/E/R	LO8030 + loxP-mCherry-bueA/B/C/D/E/R-pyrG -lox2272-72::IS1

Table S4 Oligonucleotides and gBlock used in this work.

Oligonucleotide	Sequence	Purpose
Cre-Lic-FW	TAGAGGATCACTCGTCGTGTCGCCCATGTCTAATTTGTTGACTGTTCATCAAAATT	Cloning Cre into pBargpe1
Cre-Lic-Rv	GCCCCCCCTCGAACGTCGTCGTCGCCCATCACCATCTTCCAAGAGTCTAACC	Cloning Cre into pBargpe1
RvSp_i147	ACGTCGTCGTCGCCCTAATCACCATCTTCCAAGAGTCTAACC	To build pGem-PgpdA-Cre
FwSp_147	UAGGGCGACGACGACGTTCG	To build pGem-PgpdA-Cre
i147_AW_Fw	ACCGTCCGTCTCTCCGCATGTTCACTGGCCGTCGTTTTACAAC	To build pGem-PgpdA-Cre
i147_AW_Rv	ACAGCTCATCTGCAATGCATCATGGTCATAGCTGTTTCCTGTG	To build pGem-PgpdA-Cre
TtrcRv	ATGCATTGCAGATGAGCTGTATC	To build pGem-PgpdA-Cre
PgpdA-Fw	CATGCGGAGAGACGGACGG	To build pGem-PgpdA-Cre
AattI-Lox2272-71Rv	ATTATAGATCATAACTTCGTATAAAGTATCCTATACGAACGGTAGCTAGCTGTACGT	To build pGemLP1-loxP-bar-Lox2272-71
AattI-Lox2272-71Fw	ACAGCTAGCTACCGTTCGTATAGGATACTTTATACGAAGTTATGATCTATAAT	To build pGemLP1-loxP-bar-Lox2272-71
FwUpST	TTCCTCGTCGTGTCGCCCAAGTGTAGGTAATGATTAGGATTGCTGG	To build pGemLP1-loxP-bar-Lox2272-71
RvUpST	CCGCTCATGAGACAATAACCCTGTCCCACCTTGATCTACCTGC	To build pGemLP1-loxP-bar-Lox2272-71

FwDownST	TATACATCGCAGGGGGTTGACCAAAGGTTGGGTCGTCGGTA	To build pGemLP1-loxP-bar-Lox2272-71
RvDownST	CGTCGTCGTCGCCCAGCATTGGACAGCGCGTTAAT	To build pGemLP1-loxP-bar-Lox2272-71
FwpBarLoxPLox2272	AGGGTTATTGTCTCATGAGCGG	To build pGemLP1-loxP-bar-Lox2272-71
RvpBarLoxPLox2272	GTCAACCCCCTGCGATGTATA	To build pGemLP1-loxP-bar-Lox2272-71
i150_HA2TS1_Fw	ATATTAAGGGTTCCGGATCGCGGCGGTTGATTGAGTCGAGATAGTC	To build pGemLP2-loxP-bar-Lox2272-71
i150_HA2TS1_Rv	CATATGGTCGACCTGCAGGCGGCCGCCCAAGTTGTCGGAAGGATGACC	To build pGemLP2-loxP-bar-Lox2272-71
i150_HA1TS1_Rv	TCCGCTCATGAGACAATAACCCTTTACACAGACCAGCAATCATCAAAC	To build pGemLP2-loxP-bar-Lox2272-71
i150_HA1TS1_Fw	CATGCTCCCGGCCGCCATGGCGGCCGCGGACATCTCTCATGGCTCGC	To build pGemLP2-loxP-bar-Lox2272-71
gblock 1	CATCGCCGGTCGAGGCATCTACGCTGCTCCCGACCCGGTTGAAGCTGCACAGCGGTACCAGAAAGAAGGCTGGGAAGCTTATATGGCACGTGTCTGTGGTAAAAGCTGAACTCTGATTGCTAGCCAGAACTACCGTTCGTATAAAGTATCCTATACGAAGTTATCCCTTAAGGTATATGCGGCAAGTCATGATTTCCTCTTGGAGCAAAAGTGTAGTGCCAGTACGAGTGTTGTGGAGGAAGGCTGCATACATTGTGCCT	To build pKW20088-loxP-mcherry-pyrG-lox2272-66
LoxP-pyrG-F	TAACTTCTTCGGCGACAGCATCACCGACTTCGTTAATTAATGGGCTCTGAGTGTGTTTGG	To build pKW20088-loxP-mcherry-pyrG-lox2272-66 and amplifying fragments for *in vitro* recombination

pyrG-LoxP-R	GTCTTTGGCAACACCAAACACACTCAGAGCCCATTAATTAACGAAGTCGGTGATGCTGTC	To build pKW20088-loxP-mcherry-pyrG-lox2272-66
pKW-LoxP-F	AGTAACCTCGCGGGTGTTCTTGACGATGGCATCCTGCGACGTCGACTCTAGAGGATCCCC	To build pKW20088-loxP-mcherry-pyrG-lox2272-66
PyrgPartR	GCCATATAAGCTTCCCAGCCT	To build pKW20088-loxP-mcherry-pyrG-lox2272-66
LIC-mcherry-FW	CTCGTCGTGTCGCCCATGGTGAGCAAGGGCGAGGAG	To build PgpdA-mCherry-TrpcT
LIC-mcherry-Rv	CGTCGTCGTCGCCCATTACTTGTACAGCTCGTCCATGC	To build PgpdA-mCherry-TrpcT
pacIgpdeRv	ATGTCTTTGGCAACACCAAACACACTCAGAGCCCATTAATTAACGTCATGCATTGCAGAT	To build pGem-loxp-mcherry-lox71-2272 and pKW20088-loxP-mcherry-pyrG-lox2272-66
pacIgpdeFw	TCTTAACTTCTTCGGCGACAGCATCACCGACTTCGCGATCGCATGCGGAGAGACGGACG	To build pGem-loxp-mcherry-lox71-2272 and pKW20088-loxP-mcherry-pyrG-lox2272-66
NotI-PkwF	TACATCATGCGGCCGCCACTGAGAACCATGGCACCGAAG	To build pGem-loxp-mcherry-lox71-2272
NotI-Gblock-Rv	TACTATAAGCGGCCGCCTTACCTCACTTGCTAGATGACTGG	To build pGem-loxp-mcherry-lox71-2272
PyrgTBsmbIRv	CAATCACGCATTCCCGAGTG	To build pRecomb-loxp-mcherry-4Gcloningsite-lox71-2272-66
pyrgT-mut-bsmbI-F	AATGGATACGTGCACTCGGGAATGCGTGATTGGCTCGACTCGTGTTCTCAGTTCCTCATTCC	To build pRecomb-loxp-mcherry-4Gcloningsite-lox71-2272-66
Crelox-4g-Fw	ATCTGCAATGTTAAGAATTCGCTGATTGTGATAGTTCCCACTTG	To build pRecomb-loxp-mcherry-4Gcloningsite-lox71-2272-66

Crelox-4g-Rv	CACACTCAGAGCCCAGAATTCTGATCTTCTCATCACGCCTCTTG	To build pRecomb-loxp-mcherry-4Gcloningsite-lox71-2272-66
Crelox-mche-Fw	AGATGCGTAAGGAGAGTCGACTCTAGAGGATCCCCG	To build pRecomb-loxp-mcherry-4Gcloningsite-lox71-2272-66
Crelox-mche-Rv	CACAATCAGCGAATTCTTAACATTGCAGATGAGCTGTATCTGG	To build pRecomb-loxp-mcherry-4Gcloningsite-lox71-2272-66
Crelox-ori-Fw	AGAAGATCAGAATTCTGGGCTCTGAGTGTGTTTGGTG	To build pRecomb-loxp-mcherry-4Gcloningsite-lox71-2272-66
Crelox-ori-Rv	TCCTCTAGAGTCGACTCTCCTTACGCATCTGTGCG	To build pRecomb-loxp-mcherry-4Gcloningsite-lox71-2272-66
Bur_140_Fw1	CCTCTTCCAGATACAGCTCATCTGCAATGTTAACGTGCGACCCTGAAACTACA	To build pRecomb-loxp-mcherry-BueABCDER-lox71-2272-66
Bur_Rv1	AACCGTTGGGCGACAAGG	To build pRecomb-loxp-mcherry-BueABCDER-lox71-2272-66
Bur_Fw2	AGGCTCATCTTCCTTGTCGC	To build pRecomb-loxp-mcherry-BueABCDER-lox71-2272-66
Bur_Rv2	GTCGCTCTCGATGATGGTACAC	To build pRecomb-loxp-mcherry-BueABCDER-lox71-2272-66
Bur_Fw3	CGTAGGCCGAGTGTACCATC	To build pRecomb-loxp-mcherry-BueABCDER-lox71-2272-66
Bur_Rv3	GGGTTGCCTGTCTGTCCC	To build pRecomb-loxp-mcherry-BueABCDER-lox71-2272-66

Bur_Fw4	GCGGACGTTATCTTTGGGGAC	To build pRecomb-loxp-mcherry-BueABCDER-lox71-2272-66
Bur_140Rv	TTTGGCAACACCAAACACACTCAGAGCCCAATGCTTGCGAATGGTGCACC	To build pRecomb-loxp-mcherry-BueABCDER-lox71-2272-66
HA1TS1_Scr	GGCTTGGACATCAAATGGGC	Screening PCR
HA2TS1_Scr	AACACCCTGGATTTCGTGGG	Screening PCR
BarDownstream-F-Seq	GACGTGGGTTTCTGGCAGC	Screening PCR 1
PbarUpstream-R-Seq	GCATTCATTGTTGACCTCCACTAGC	Screening PCR 2
Gblock-R	CTTACCTCACTTGCTAGATGACTGG	Amplifying fragments for *in vitro* recombination
P1FwUpST	GACGACGAATACTATGCATCCTTG	Screening PCR 2 and 4 (LP1)
P6RVDownST	CAGAGGACCCCAGGAACGA	Screening PCR 1 and 3 (LP1)
RMCEgpda_Fw	CCGGGTACTCGCTCTACCTAC	Screening PCR 3
RMCEpyrg_RV	TCCAAAGGATCGCTGGCTAC	Screening PCR 4

References

1. Hu, J., Sarrami, F., Li, H., Zhang, G., Stubbs, K. A., Lacey, E., Stewart, S. G., Karton, A., Piggott, A. M. M., & Chooi, Y.-H. H. (2019). Heterologous biosynthesis of elsinochrome A sheds light on the formation of the photosensitive perylenequinone system. *Chemical Science*, *10*, 1457–1465. https://doi.org/10.1039/c8sc02870b

2. Chiang, Y. M., Ahuja, M., Oakley, C. E., Entwistle, R., Asokan, A., Zutz, C., Wang, C. C. C., & Oakley, B. R. (2016). Development of Genetic Dereplication Strains in *Aspergillus nidulans* Results in the Discovery of Aspercryptin. *Angewandte Chemie - International Edition*, *55*, 1662–1665. https://doi.org/10.1002/anie.201507097